



Original article

Novel isatinyl thiosemicarbazones derivatives as potential molecule to combat HIV-TB co-infection

Debjani Banerjee, Perumal Yogeeswari, Pritesh Bhat, Anisha Thomas, Madala Srividya, Dharmarajan Sriram*

Medicinal Chemistry & Antimicrobial Research Laboratory, Pharmacy Group, Birla Institute of Technology & Science—Pilani, Hyderabad Campus, Jawahar Nagar, Hyderabad-500 078, Andhra Pradesh, India

ARTICLE INFO

Article history:

Received 16 July 2010

Received in revised form

19 October 2010

Accepted 20 October 2010

Available online 27 October 2010

Keywords:

Isatin

Mannich base

HIV-TB co-infection

Isocitrate lyase

ABSTRACT

A series of novel 5-substituted-1-(arylmethyl/alkylmethyl)-1H-indole-2,3-dione-3-(N-hydroxy/methoxy thiosemicarbazone) analogues were synthesized and evaluated for their anti-HIV activity and anti-tubercular activity in both log phase and starved cultures. The compound 2-(1-([4-(4-chlorophenyl)tetrahydropyrazin-1(2H)-yl]methyl)-5-methyl-2-oxo-1,2-dihydro-3H-indol-3-yliden)-N-(methyloxy)hydrazine-1-carbothioamide (**B21**) displayed promising activity against the replication of HIV-1 cells (EC_{50} 1.69 μ M). In anti-mycobacterial screening **B21** proved effective in inhibiting the growth of both log phase (MIC 3.30 μ M) and starved (MIC 12.11 μ M) MTB cultures. Isocitrate lyase enzyme having momentous implication in persistent TB was shown to be inhibited by 1-cyclopropyl-6-fluoro-7-[4-([5-methyl-3-((Z)-2-((methyloxy)amino)carbothioyl]hydrazono)-2-oxo-1H-indol-1(2H)-yl]methyl)tetrahydropyrazin-1(2H)-yl]-4-oxo-1,4-dihydroquinoline-3-carboxylic acid (**B30**) with 63.44% inhibition at 10 mM.

© 2010 Elsevier Masson SAS. All rights reserved.

1. Introduction

The acquired immunodeficiency syndrome (AIDS) has acquired pandemic proportion globally and has claimed more lives than any other diseases. According to the 2008 UNAIDS report released by the WHO, 33 million people were diagnosed to be human immunodeficiency virus (HIV)-positive in 2007 [1]. The 2008 WHO report on tuberculosis (TB), states that 0.7 million cases of HIV-TB co-infection were reported in 2006 and an estimate of 0.2 million of the global populace died due to HIV-TB co-infection [2]. TB and HIV have a harmonized effect on the progression of each other and hence become a lethal threat to the patient. The therapy available for treating patients co-infected with HIV and TB involves a very high pill burden, which reduces the chances of treatment adherence by the subjects. Current combination therapy for treating patients co-infected with HIV & TB involves non-nucleoside reverse transcriptase inhibitors (NNRTI) viz. efavirenz, nevirapine, delaviridine and viral protease inhibitors viz. nelfinavir, ritonavir, saquinavir and a combination regimen comprising of rifampicin (RIF), isoniazid (INH), ethambutol and pyrazinamide to combat the tubercle bacilli.

As stated in a recent review by Pepper et al., dire consequences arise due to drug–drug and drug–disease interactions and a paradoxical aggravation of tuberculous pathologies occur due to reconstitution of immunity while treating the patients with combination anti-retroviral and anti-tubercular therapies [3,4]. In patients who have been exposed to the tubercle bacilli, the chances that the bacilli persist in a dormant state in the lungs are very high which can lead to reactivation tuberculosis. This dormant/latent TB evades immunity and also presents itself as an elusive target by the existing anti-tubercular therapies [5]. Sacchetti et al., in 2000 reported that isocitrate lyase (ICL), a significant enzyme in the glyoxalate shunt plays a crucial role in the persistence of MTB in the macrophages and escapes immunity [6].

Isatin derivatives have been long reported for their anti-viral activities specifically for their action against pox virus [7], vaccinia [8], rhino virus [9], moloney leukemia virus [10] and sars [11] viruses. Previous works have also reported the inhibitory activity of isatin- β -thiosemicarbazones and isatin derivatives on HIV replication [12–15]. In this paper, we have reported the synthesis of sixty diverse N-Mannich base derivatives of 3-(N-hydroxy/methoxy thiosemicarbazones) of 5-substituted isatins as potential NNRTI which also inhibited the ICL enzyme of MTB thereby tackling the issues of dormant tuberculosis, which often presents itself as an opportunistic infection (OI) in patients afflicted with AIDS. Thus we hypothesize that these new molecules would bypass the pharmacokinetic

* Corresponding author. Tel.: +91 9010534101; fax: +91 40 66303998.

E-mail addresses: dsriram@bits-hyderabad.ac.in, drdsriram@yahoo.com (D. Sriram).

interferences of combination HIV-TB therapy, tackle the consequences arising due to immune reconstitution and also minimize the pill burden thereby increasing the prospects of patient compliance.

2. Chemistry

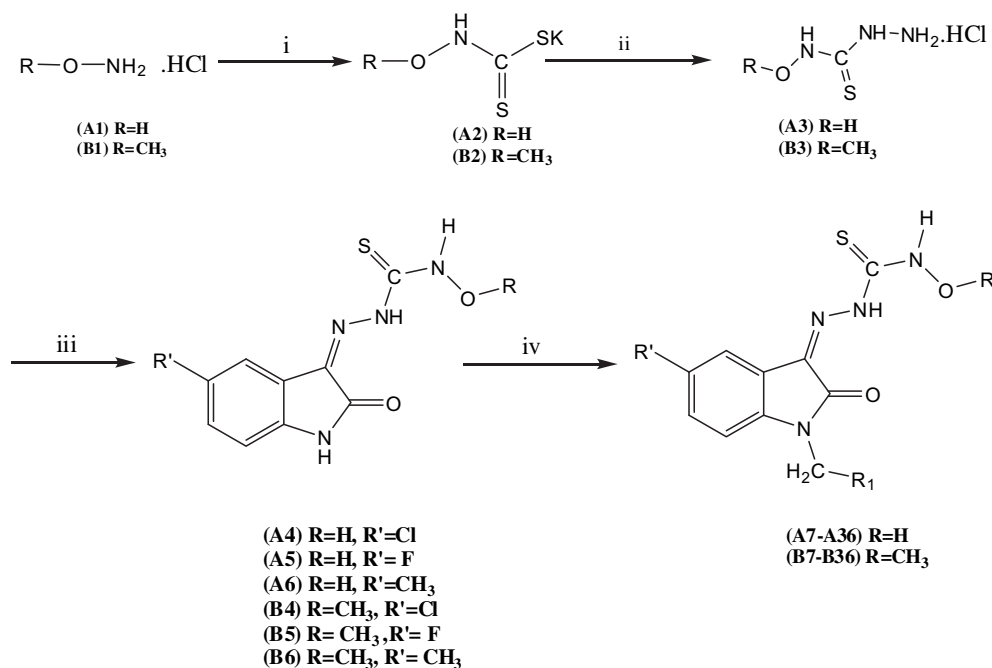
The synthesis of the titled compounds of series **A** (**A7–A36**) and series **B** (**B7–B36**) was accomplished in four steps and is outlined in Scheme 1 [16]. When an equimolar amount of N-hydroxylamine hydrochloride/N-methoxyamine hydrochloride and carbon disulfide were added to an ethanolic solution of potassium hydroxide it yielded the potassium hydroxy/methoxy dithiocarbamates, which when further reacted with hydrazine hydrate generated the respective thiosemicarbazide hydrochloride salts as fine needle shaped yellow crystals. This intermediate was further condensed with various substituted isatins under the conditions of Schiff reaction in the presence of sodium acetate, which yielded the corresponding Schiff bases. The N-Mannich bases were synthesized further by condensing the acidic imino group of isatin derivatives with formaldehyde and various secondary amines by irradiating the reaction vessel in a scientific microwave reactor for 3–15 min at 455 W. This reaction was also conducted parallelly using conventional technique, but the reaction took sixty to 72 h to attain completion; whereas when the reaction was carried out under microwave irradiation, reaction time was considerably shortened and yield was also enhanced. Moreover microwave technique is greener since it requires solvent in negligible amounts and it also obviates the need for work-up.

Elemental and spectral analyses were also performed to assess the purity of the compounds. IR spectra in general showed an azomethine (C=N) peak at 1620 cm^{-1} and methylene (Mannich) peak at 2840 cm^{-1} . In the ^1H NMR spectra the signals of the respective protons of the synthesized compounds were confirmed based on their chemical shifts, multiplicities and coupling constants. These spectra showed a singlet at 4.9–5.3 ppm, which corresponds to the $-\text{NCH}_2\text{N}$ protons. Elemental analyses results were within $\pm 0.4\%$ of the theoretical values.

3. Biological results and discussion

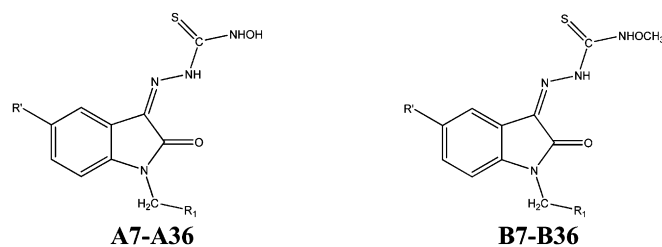
3.1. In-vitro anti-HIV assays

The titled compounds were tested for their ability to inhibit the replication of HIV-1 (III_B) cells in MT-4 cells. All the sixty analogues had EC_{50} lying in the range of $1.69\text{ }\mu\text{M}$ – $129.96\text{ }\mu\text{M}$ (Table 1). Fifteen derivatives had EC_{50} less than $10\text{ }\mu\text{M}$. Amongst the thirty hydroxy thiosemicarbazone derivatives **A35** was found to be the most promising with EC_{50} of $4.18\text{ }\mu\text{M}$. Amongst the various substituted piperazinyl analogues the most potent ones were found to be the 4-chlorophenyl piperazinyl derivatives (**A19–A21**) followed by 4-methoxyphenyl piperazine (**A22–A24**) and then phenyl piperazine (**A16–A18**) derivatives. The presence of dialkylamine at R_1 ruled anti-HIV activity by the following order: N,N-diethylamine > N,N-dimethylamine. When R_1 was substituted by various fluoroquinolones (FQ), gatifloxacin analogues (**A34–A36**) showed the greatest inhibition of HIV replication followed by lomefloxacin derivatives (**A31–A33**) and then by ciprofloxacin (**A28–A30**) and norfloxacin analogues (**A25–A27**) which were almost equipotent to each other. The methoxy thiosemicarbazone analogues when compared to those of hydroxy thiosemicarbazone derivatives displayed better inhibitory profile. The higher activity of the methoxy thiosemicarbazones in comparison to the hydroxy thiosemicarbazones can be attributed to the methoxy moiety, being involved in steric interaction with the aromatic residues of HIV-1 RT; which was confirmed with the docking results obtained. In the series of methoxy thiosemicarbazone analogues, 2-(1-([4-(4-chlorophenyl) tetrahydropyrazin-1(2H)-yl] methyl)-5-methyl-2-oxo-1,2-dihydro-3H-indol-3-yliden)-N-(methoxy)hydrazine-1-carbothioamide (**B21**) was found to be the most potent in suppressing the replication of HIV-1 cells with an EC_{50} of $1.69\text{ }\mu\text{M}$. The anti-HIV potency of **B21** may be ascribed to the electronegative chlorine present at the 4th position of phenyl piperazinyl methyl which probably forms a lipophilic interaction in the active site pocket and also owing to the methyl group at the 5th position of the indolyl moiety which helps it in establishing lipophilic



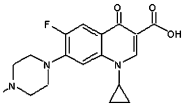
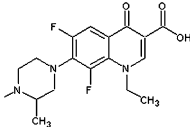
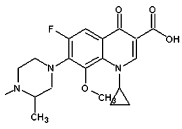
Scheme 1. Synthetic protocol of compounds. Reagents & Conditions: (i) CS_2 , KOH, $\text{C}_2\text{H}_5\text{OH}$, $0-5\text{ }^\circ\text{C}$, 0.5 h; (ii) $\text{NH}_2\text{NH}_2\cdot\text{H}_2\text{O}$, $80\text{ }^\circ\text{C}$, 1 h, conc. HCl; (iii) 5-R'-isatin ($\text{R}' = \text{Cl}, \text{F}, \text{CH}_3$), CH_3COONa ; (iv) 30% HCHO, NHR₁, M.W.I, 455 W, 3–15 min.

Table 1
Physical Constants, anti-HIV activity and anti-tubercular activity of **A7–36**, **B7–36**.



Sl. No.	R'	R ₁	M.P(°C)	% yield	HIV-1		MTB MIC ^c (μM)
					EC ₅₀ ^a (μM)	CC ₅₀ ^b (μM)	
A7	Cl	—N(CH ₃) ₂	102–104	97.05	129.96	610.15	76.27
B7	Cl	—do—	60–62	98.28	57.93	551.75	18.28
A8	F	—do—	40–42	87.10	47.22	599.15	10.05
B8	F	—do—	56–58	82.45	37.80	559.69	9.62
A9	CH ₃	—do—	110	95.85	113.22	650.68	81.34
B9	CH ₃	—do—	82–84	93.45	64.09	622.28	19.45
A10	Cl	—N(C ₂ H ₅) ₂	125–127	98.61	120.84	562.05	70.26
B10	Cl	—do—	52–54	69.28	58.40	454.21	16.90
A11	F	—do—	80–82	79.90	36.24	520.93	9.22
B11	F	—do—	98–100	83.50	29.71	490.07	4.41
A12	CH ₃	—do—	114–116	71.47	57.61	534.25	11.83
B12	CH ₃	—do—	88–90	68.81	53.27	572.80	8.96
A13	Cl		46–48	56.43	35.13	347.72	6.11
B13	Cl	—do—	72–74	98.90	28.40	322.26	4.06
A14	F	—do—	36–38	64.75	61.41	465.01	4.41
B14	F	—do—	80–84	89.53	28.85	274.09	4.25
A15	CH ₃	—do—	58–62	64.47	93.59	572.39	8.96
B15	CH ₃	—do—	86–90	75.70	45.13	365.41	4.29
A16	Cl		148–150	87.21	28.32	273.07	28.09
B16	Cl	—do—	80–82	93.33	17.65	267.13	13.62
A17	F	—do—	78–80	86.09	19.60	250.89	7.30
B17	F	—do—	108–110	79.94	18.08	226.89	7.07
A18	CH ₃	—do—	68–70	79.93	19.32	420.00	14.72
B18	CH ₃	—do—	87–89	83.57	17.3	276	12.36
A19	Cl		110–112	92.40	11.06	268.14	13.04
B19	Cl	—do—	208–210	74.26	2.43	228.61	6.34
A20	F	—do—	72–74	73.50	6.85	193.55	3.37
B20	F	—do—	202	76.87	3.77	346.79	3.27
A21	CH ₃	—do—	178–182	76.34	6.10	335.11	6.82
B21	CH ₃	—do—	140	85.46	1.69	300.22	3.30
A22	Cl		140	58.32	21.26	278.76	13.16
B22	Cl	—do—	108–110	73.92	13.09	220.86	12.78
A23	F	—do—	54–56	60.38	14.66	259.54	6.83
B23	F	—do—	116–118	69.35	12.7	276	6.14
A24	CH ₃	—do—	216–218	88.66	14.96	320.98	13.75
B24	CH ₃	—do—	98–102	61.11	9.82	324.39	6.68
A25	Cl		166–168	71.55	27.24	185.54	1.30
B25	Cl	—do—	170–174	98.59	19.15	192.51	0.65
A26	F	—do—	88–90	72.88	18.44	207.66	1.33
B26	F	—do—	66–68	93.50	10.51	143.76	0.67
A27	CH ₃	—do—	180–182(d)	47.33	16.88	326.67	1.34

Table 1 (continued).

Sl. No.	R'	R ₁	M.P(°C)	% yield	HIV-1		MTB MIC ^c (μM)
					EC ₅₀ ^a (μM)	CC ₅₀ ^b (μM)	
B27	CH ₃	-do-	158–162(d)	67.23	11.42	237.72	1.31
A28	Cl		210(d)	92.05	33.38	229.30	2.54
B28	Cl	-do-	128–130(d)	72.53	10.99	142.66	0.64
A29	F	-do-	230(d)	90.62	16.50	222.23	0.33
B29	F	-do-	184(d)	65.08	11.43	254.78	0.31
A30	CH ₃	-do-	40	71.67	20.89	303.72	0.67
B30	CH ₃	-do-	150–154(d)	85.67	9.22	231.71	0.66
A31	Cl		226–228	88.59	23.18	209.45	1.23
B31	Cl	-do-	>230	48.33	9.26	180.38	1.20
A32	F	-do-	130(d)	61.75	9.93	186.85	0.65
B32	F	-do-	180(d)	72.90	4.43	178.27	0.63
A33	CH ₃	-do-	140–144	72.36	11.73	243.95	0.65
B33	CH ₃	-do-	206–210(d)	81.22	5.74	155.50	1.24
A34	Cl		136–138	90.92	15.35	233.73	1.19
B34	Cl	-do-	154–156	8.47	7.14	164.25	0.30
A35	F	-do-	70–74	66.79	4.18	205.88	0.16
B35	F	-do-	88–90	70.23	1.88	170.51	0.15
A36	CH ₃	-do-	70	77.75	11.13	276.00	0.63
B36	CH ₃	-do-	70–72	46.09	1.86	154.06	0.31
Nevirapine	—	—	—	—	0.13	156	—
Troviridine	—	—	—	—	0.016	87	—

^a Effective concentration of the drug that reduces HIV-1 induced cytopathic effect by 50% in MT-4 cells.^b Cytotoxic concentration of the drug that decreases MT-4 cell's viability by 50%.^c MIC was the concentration at which the H₃₇Ra MTB strain showed complete inhibition.

interactions with aromatic residues of the enzyme. Between morpholinyl and piperazinyl substitution at R₁ of the methoxy thiosemicarbazones, piperazinyl analogues (**B16–B24**) showed improved anti-HIV potency. Comparison between the various substituted piperazinyl showed that 4-chlorophenyl piperazine derivatives (**B19–B21**) were most active followed by 4-methoxyphenyl piperazine (**B22–B24**) and lastly phenyl piperazinyl analogues (**B16–B18**). 4-Chlorophenyl piperazinyl methyl substituted molecules showed higher inhibitory activity against replication of HIV-1 cells in comparison to other phenyl piperazines namely phenyl piperazine and 4-methoxyphenyl piperazine due to the halogen group present at the 4th position of the phenyl ring forming a bond with some positively charged residues of the RT enzyme. Presence of various FQs at R₁ guides activity in the following sequence: gatifloxacin > lomefloxacin > ciprofloxacin ≈ norfloxacin. The presence of FQs at N-1 makes the molecule **B36** the second most potent molecule amongst the total 60 reported compounds against HIV replication. When considering the substituent at 5th position of the indole-2,3-dione it was observed that activity was governed by the order of F ≈ CH₃ > Cl. Compounds with N, N-diethylaminomethyl substitution at N-1 of indole-2,3-dione (**A10–B12**) showed better inhibitory activity than those with N,N-dimethylamine methyl substitution (**A7–B9**) possibly due to the longer aliphatic chain length

contributing to improved interaction with the bulky groups present at the active site. Substitution at R₁ also ruled the pattern of activity followed by the compounds. Presence of piperazinyl methyl and substituted piperazinylmethyl group at N-1 enhanced the anti-HIV activity when compared to morpholinylmethyl group. This can be attributed to the repulsion experienced by the oxygen of morpholine ring.

The cytotoxic effect of these molecules was measured in MT-4 cells in parallel with the anti-viral activity. Amongst the entire series **A9** was found to be least cytopathic to MT-4 cells with a CC₅₀ value of 650.68 μM. The CC₅₀ values of the entire series of sixty compounds were found to lie in the range of 143.76–650.68 μM (Table 1). When compared to standard non-nucleoside reverse transcriptase inhibitors (NNRTI) like nevirapine and delaviridine, which have CC₅₀ of around 25 μM, these new molecules are far less cytotoxic. Cytotoxicity was found to be regulated by the occurrence of greater bulky groups at N-1 of indolyl moiety. While comparing between the terminal substituent present at the hydrazino carbothioamide it was seen that molecules belonging to series of methoxy thiosemicarbazone analogues were mostly less toxic than that of the series of hydroxythiosemicarbazones except for a few isolated cases, which can be ascribed to the probable hydrogen bond formation by the hydroxyl group with residues of the MT-4 cells.

3.2. HIV-1 RT enzyme inhibition assay

HIV-1 reverse transcriptase (RT) is a predominant target for many anti-HIV drugs that are being used clinically and are there in the developmental stages. RT is a multifunctional heterodimeric enzyme needed in HIV replicative cycle, which catalyzes the conversion of genomic HIV RNA into proviral DNA [17,18]. Drugs targeting RT are classified into two broad categories: nucleoside reverse transcriptase inhibitors (NRTI) and non-nucleoside reverse transcriptase inhibitors (NNRTI). NNRTIs inhibit RT in a non-competitive manner by binding at an allosteric site that is situated 10 Å away from the catalytic HIV-RT site [19]. NNRTIs are specific to HIV-1 RT and hence are comparatively less toxic to the host. Though NNRTIs are structurally diverse, they act on RT by inducing conformational changes that form the NNRTI binding pocket (NNIBP). They achieve this by distorting the polymerase active site by means of movement of the catalytic aspartates [20].

Four compounds were assessed for their activity against wild type HIV-1 RT. Compound **B21** showed the highest inhibitory activity with IC_{50} of $11.5 \pm 1.5 \mu M$ (Table 2) on HIV-1 RT amongst all four, which can be ascribed to the methyl moiety present at thiosemicarbazone moiety, which may be involved in lipophilic interaction with some residues present in the RT active site. Activity can moreover be guided by the phenyl ring attached to the piperazinyl moiety at R_1 , which can contribute to significant interaction with aromatic residues of the RT enzyme as is evident from the docking simulations performed.

3.3. In-vitro anti-tubercular evaluation

The titled compounds when evaluated for their inhibitory activity against the replication of MTB in the logarithmic growth phase displayed activity ranging from 0.15 to $81.34 \mu M$ (Table 1). Forty-four compounds had minimum inhibitory concentrations (MIC) below $10 \mu M$ out of which fifteen molecules' MIC were found to lie below $1 \mu M$. 1-Cyclopropyl-6-fluoro-7-[4-[[5-fluoro-3-((Z)-2-[(methoxy)amino]carbothioyl)hydrazono]-2-oxo-1H-indol-1(2H)-yl]methyl]-3-methyltetrahydropyrazin-1(2H)-yl]-8-(methoxy)-4-oxo-1,4-dihydroquinoline-3-carboxylic acid (**B35**) was found to be the most active against the logarithmic growth of MTB with MIC of $0.15 \mu M$, even more potent than INH (MIC: $0.36 \mu M$). In contrast to the hydroxy thiosemicarbazone analogues, the methoxy thiosemicarbazones exhibited superior activity against MTB growth. Amongst the hydroxy thiosemicarbazone analogues the most active compound was found to be **A35** with an MIC of $0.16 \mu M$ (Table 1). Keeping R' constant in the hydroxysemicarbazone series when R_1 was varied the order of activity was as follows: N,N-dimethylamino < N,N-diethylamino < phenyl piperazinyl < 4-methoxyphenyl piperazinyl < 4-chlorophenyl piperazinyl < morpholinyl < norfloxacin < ciprofloxacin < lomefloxacin < gatifloxacin. Substituents at R' influenced the anti-tubercular activity in the following order:

Table 2

HIV-1 RT enzyme Inhibition Data for Substituted Isatin- β -thiosemicarbazones^a.

Compd	IC_{50} (μM) against HIV-1 RT ^b
A21	23.4 ± 1.2
B19	18.3 ± 2.1
B20	16.7 ± 2.3
B21	11.5 ± 1.5
Nevirapine	0.25
Troviridine	0.017 ± 0.007

^a Enzyme assays done with WT RT.

^b IC_{50} is the quantity of drug that reduced WT RT enzyme activity by 50%.

fluorine > chlorine \approx methyl, with moderate to lowest activity swaying between chlorine and methyl, which might be due in part to the combined effect of the substituent present at R_1 .

Compound **B35** was found to be the most promising in the methoxy thiosemicarbazone series. Varying substituents at R_1 led to the same order of activity as that of hydroxy thiosemicarbazones. The greater activity profile of the fluoroquinolone-substituted analogues (**A25–B36**) can be accredited to their increased lipophilicity permitting them to penetrate into the mycolic acid cell wall of the bacilli. In case of the morpholinyl derivatives (**A13–B15**) the enhanced activity in contrast to the piperazinyl derivatives may be due in part to the electronegative oxygen which might be involved in some ionic interaction or some hydrogen bonding interaction with residues at the active site. Amongst the substituted piperazinyl analogues, the 4-chlorophenyl piperazinyl analogues demonstrated highest activity, which can be attributed to the chlorine atom being involved in some probable ion–dipole interaction with the residues of the active site pocket. In the presence of dialkylamino group at R_1 , increased alkyl chain length contributed to greater inhibition of MTB replication possibly due to increased lipophilic factor. These results were further established by the docking simulations that were performed.

These compounds also showed exemplary inhibitory profile against starved MTB culture. Twenty compounds from amongst the sixty derivatives were tested for their activity against the replication of dormant MTB culture (Table 3). Compound **B35** proved superior in curbing the growth of dormant MTB (MIC: $9.17 \mu M$) in comparison to first-line anti-tubercular drugs, INH (MIC: $182.31 \mu M$) and RIF (MIC: $15.19 \mu M$). All the twenty analogues were found to be more active (MIC ranging from 9.17 to $42.11 \mu M$) in suppressing the proliferation of dormant MTB when compared to INH. Seven of them were found to be more beneficial (MIC ranging from 9.17 to $13.48 \mu M$) than RIF in inhibiting dormant MTB.

3.4. MTB ICL enzyme inhibition assay

In chronic TB, the bacillus exists in diverse metabolic phases, spanning from active cell growth to stationary phase [13]. All the currently available anti-tubercular drugs that are being clinically

Table 3

Comparison between anti-tubercular activity of selected compounds against log phase and dormant MTB.

Compd	MTB in log phase (μM)	Dormant MTB (μM)
A20	3.37	13.48
A21	6.82	27.28
A29	0.33	20.92
A30	0.67	42.11
A32	0.65	10.12
A33	0.65	20.37
A35	0.16	9.74
A36	0.63	19.60
B14	4.25	17.01
B19	6.34	25.36
B20	3.27	13.08
B21	3.30	12.11
B24	0.30	38.01
B25	0.65	36.86
B26	0.67	19.24
B28	0.64	34.62
B30	0.66	18.44
B32	0.63	9.45
B35	0.15	9.17
B36	0.31	17.81
Isoniazid	0.36	182.31
Rifampicin	0.12	15.19

used do not target various stages that MTB uses for its persistence in the macrophages and hence prolonging the treatment regimen. A lot of research activity is currently aimed at understanding the biology of persistence of the tubercle bacillus and developing new drugs that target the persister bacteria [21]. Among the gene products involved in mycobacterial persistence, isocitrate lyase (ICL) [22] could be good targets for the development of drugs that target persistent bacilli. As the compounds reported in this article, demonstrated excellent activity against dormant mycobacterium, we decided to explore the possible mechanism by screening some compounds against ICL enzyme of MTB. Several small-molecule inhibitors have been described [23] as MTB ICL inhibitors; however, none has been developed as a drug for MTB. In this work, isocitrate lyase activity was determined at 37 °C by measuring the formation of glyoxylate-phenylhydrazine in the presence of phenylhydrazine and isocitrate lyase at 324 nm based on the method described [24]. The compounds were screened with a single concentration of 10 μ M and percentage inhibitions of the screened compounds along with the standard MTB ICL inhibitor 3-nitropropionic acid (3-NP) (at 100 μ M) for comparison are reported (Table 4).

Among nine compounds which were assessed for their ability to inhibit ICL of MTB, **B30** demonstrated excellent inhibitory action of the ICL enzyme of about 63.44% and was more potent than standard ICL inhibitors like 3-NP. Compounds **B20** and **B24** showed mild ICL inhibition with range of 20–30%. Amongst the hydroxy thiosemicarbazone analogues evaluated, **A20** showed an inhibition of 18.54%. The inhibitory activities of **B24** and **B30** can be assigned to the methyl group present at R' and also to the bulky groups present at R₁, which might be contributing to significant lipophilic interaction with bulky residues present in the enzyme active pocket. This was also confirmed by the docking study performed.

4. Molecular modeling analysis

4.1. CoMFA and CoMSIA analyses based on HIV-1 screening

The CoMFA analysis was performed by dividing the array of compounds into training set of 34 compounds for model development and test set of 20 analogues, which were used for validation of this model. CoMFA study was developed using steric and electrostatic fields as independent variable and pEC₅₀ as dependent variable. CoMSIA study was developed based on steric, electrostatic, hydrophobic, hydrogen bond donor and hydrogen bond acceptor similarity fields as independent variables and pEC₅₀ as dependent variable.

The final CoMFA model was generated using cross-validated PLS analysis. PLS analysis showed a high q^2 value of 0.642 at 6 components with parabolic field (advanced CoMFA). The other fields like the indicator field and H-bonding field showed q^2 of 0.586 and 0.356 at 4 and 6 components respectively. When all these regions were focused, the q^2 improved and the parabolic field

produced the highest q^2 of 0.666 at 6 components with high conventional r^2 . The obtained model was statistically significant as was evident from the q^2 , s_{press} , SE, F -value and r^2_{bs} values tabulated in the table for CoMFA and Advanced CoMFA fields. This final CoMFA model, had a cross-validated r^2 (q^2) of 0.666 with 6 principal components. The non cross-validated r^2 was determined to be 0.955 with standard error of estimate (SE) being 0.108 and covariance ratio (F) being 99.186 (significant at 99% level). This model was further validated using the test set compounds, which confirmed its reliable predictive ability. Bootstrapping results also supported the reliability of this model. The statistical parameters of this model are listed in Table 5.

In the CoMFA model, the steric and electrostatic field contributions were 0.669 and 0.331 respectively. The steric and electrostatic contour maps of this model are shown in Fig. 1A and B respectively. The red regions in the contour maps refer to the electrostatically favored region and the blue region corresponds to electrostatically un-favored region. The green polyhedral regions correspond to sterically favored regions and yellow region refer to the sterically un-favored region. The red region near the *para* position of the phenyl ring of the phenyl piperazinyl methyl moiety suggests that introduction of more electronegative group at this position would enhance the anti-HIV activity of this class of compounds by virtue of some strong electrostatic interactions. The blue regions near the 5th and 6th carbons of the phenyl ring indicate that presence of any electronegative moiety at these positions would be detrimental for anti-viral activity. The blue polyhedra around C₇ of isatin and C₂ of piperazine also indicated that introduction of any electronegative group at these positions would diminish the potential of these compounds to inhibit HIV. In the steric contour maps the green contour zone around *para* position of phenyl ring depicts that bulkier groups would enhance the anti-HIV activity. The diminutive green polyhedra near the methoxy group attached to the thiourea revealed that introduction of moderate bulky groups would be beneficial for anti-HIV activity. The yellow region near the methyl group at C₅ of isatin demonstrates that presence of bulky substituents would negatively influence the anti-HIV profile.

The best CoMSIA model, with q^2 of 0.823 is the one when all steric, electrostatic, hydrophobic, acceptor and donor fields were taken into account, and the contributions by these fields were 0.123, 0.241, 0.329, 0.242 and 0.064 respectively (Table 5). The donor field being comparatively insignificant was ignored for further calculations. The CoMSIA hydrogen bond acceptor contour illustrates (Fig. 2B) that presence of hydrogen bond acceptor groups (magenta colored) at the position adjacent to the thiourea moiety,

Table 4
MTB ICL suppression by selected compounds.

Compound code	MTB ICL % Inhibition
A20	18.54 (10 mM)
A21	11.03 (10 mM)
B12	18.9 (10 mM)
B14	15.93 (10 mM)
B19	6.38 (10 mM)
B20	28.37 (10 mM)
B21	9.49 (10 mM)
B24	23.3 (10 mM)
B30	63.44 (10 mM)
3-NPA	65.99 (100 mM)

Table 5
Summary of CoMFA, Advanced CoMFA and CoMSIA results.

Parameters	CoMFA			CoMSIA
	SCT(RF)	PBL	PBL(RF)	SEADH
q^2	0.71	0.642	0.666	0.823
s_{press}	0.262	0.290	0.280	0.209
r^2	0.970	0.971	0.955	0.970
SE	0.089	0.086	0.108	0.088
F	148.08	156.397	99.186	151.306
N	6	6	6	9
<i>fractions</i>				
S	0.653	0.669	0.954	0.123
E	0.347	0.331	0.046	0.241
H	—	—	—	0.329
A	—	—	—	0.242
D	—	—	—	0.064
r^2_{bs}	0.984	0.986	0.978	0.981
SD_{bs}	0.007	0.003	0.007	0.005
r^2_{cv}	0.694	0.661	0.632	0.792

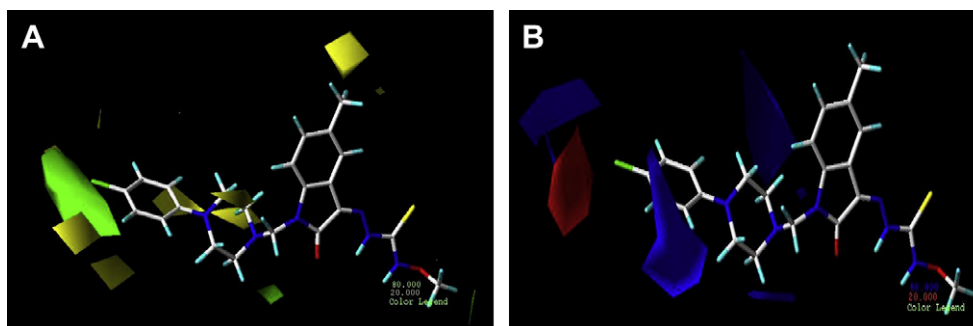


Fig. 1. A: CoMFA contour map of steric regions (green, favored; yellow; disfavored) around **B21**; B: CoMFA contour map of electrostatic regions around **B21**. Blue regions are favored by positively charged groups and red regions favored by negatively charged groups. (For interpretation of the references to color in this figure legend, the reader is referred to the web version of this article).

around the piperazine moiety and the phenyl ring attached to the piperazine ring are conducive for the anti-retroviral activity of this series. The CoMSIA hydrophobic contour map (Fig. 2A) depicted that presence of more hydrophobic moieties around the phenyl ring of isatin, piperazine and surrounding the phenyl appended to the piperazinyl methyl groups would prove to increase anti-HIV activity. The yellow polyhedron, in the CoMSIA steric contour, (Fig. 2C) near the chlorine attached to the *para* position of phenyl ring and C₅ of phenyl ring demonstrates that presence of bulky groups at these positions would hinder anti-viral activity. The green region around C₁, C₂ and C₆ of phenyl ring emphasizes that bulky groups at these positions would further enhance the anti-HIV activity. The CoMSIA electrostatic contour map (Fig. 2D) demonstrated that presence of electronegative group at *para* position of the phenyl ring would further increase the anti-retroviral activity as evident by the red region.

4.2. Docking simulation

4.2.1. HIV-1 RT docking

In order to probe the binding mode of our newly synthesized compounds in the HIV-RT active site, a modeling study was performed by means of GOLD for docking. Compound **B21** was docked onto the active site pocket of HIV-1 RT, the coordinates of which were taken from the crystal structure of RT/Nevirapine complex. The docking view of **B21** (Fig. 3A and C), exhibited that the NH moiety of the methoxythioamido group was engaged in a hydrogen bonding interaction with the ring nitrogen of Pro 140. The nitrogen of the terminal N-methoxy group was hydrogen bonded to the alcoholic oxygen of Tyr 181. The oxygen atom of the methoxy group was hydrogen bonded to the nitrogen of Gln 182's amide. The oxygen at C₂ of the indole ring was involved in hydrogen bond formation with the backbone nitrogen of Gln 91. The thioamido sulfur formed

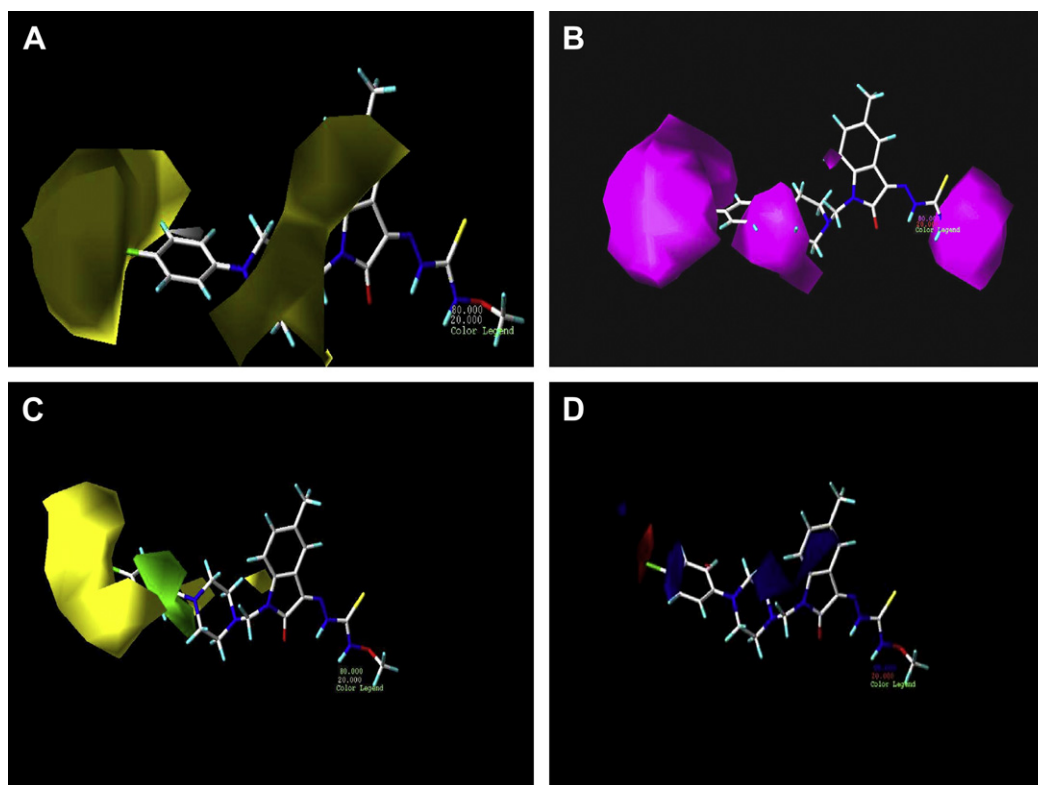


Fig. 2. A: CoMSIA contour map of hydrophobic regions (yellow favored; white disfavored) around **B21**; B: CoMSIA hydrogen bonding acceptor contour map (magenta favored; green disfavored) around **B21**; C: CoMSIA steric contour map (green favored; yellow disfavored) around **B21**; D: CoMSIA electrostatic contour map around (red favored; blue electro-negative) **B21**. (For interpretation of the references to color in this figure legend, the reader is referred to the web version of this article).

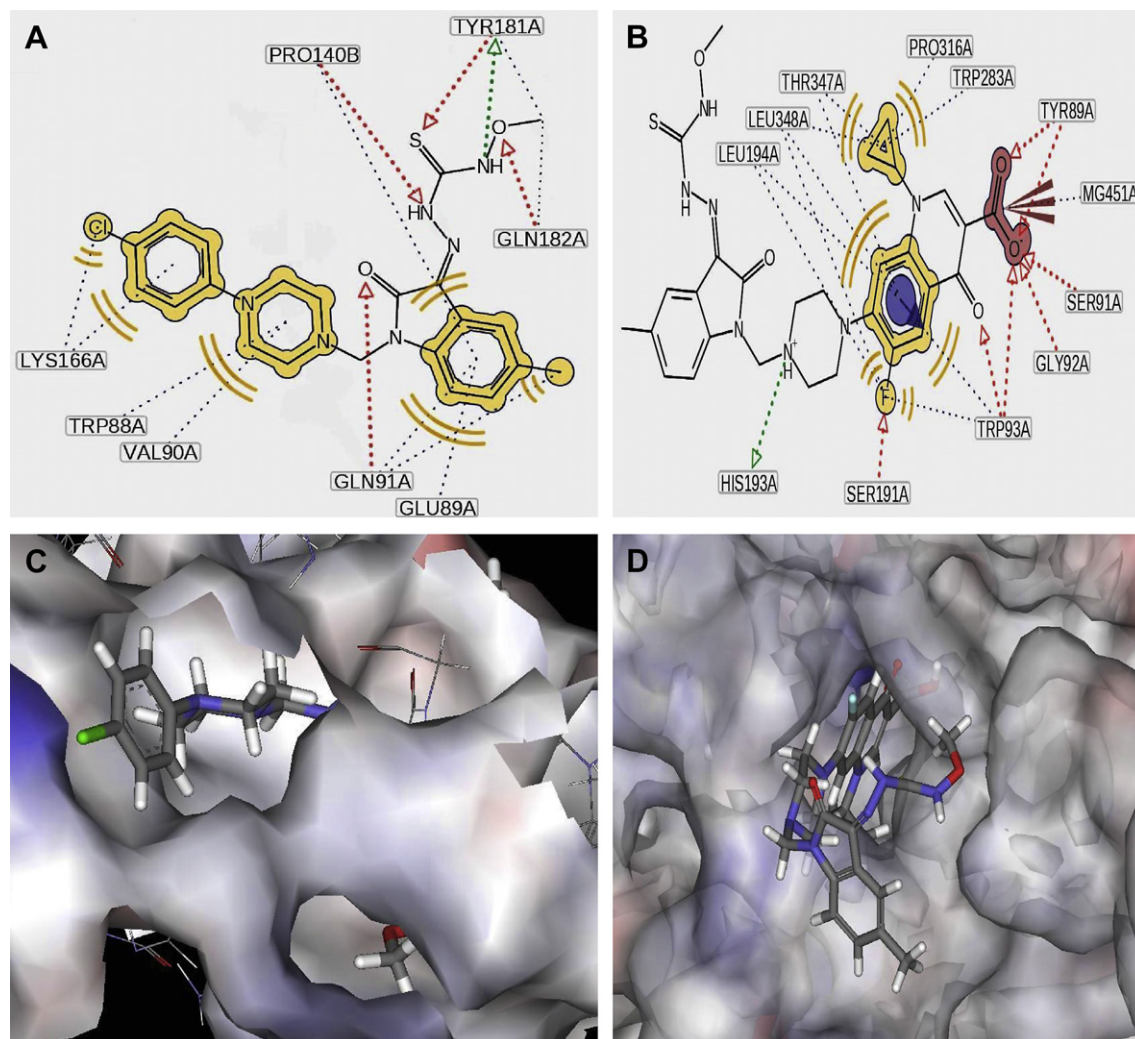


Fig. 3. A: Contact residues of **B21** when docked onto HIV-1 RT; B: Contact residues of **B30** when docked onto MTB ICL; C: Electrostatic surface view of active site pocket of HIV-1 RT bound to **B21**; D: Electrostatic surface view of active site pocket of MTB ICL bound to **B30**.

a hydrogen bond with Tyr 181. The chlorine functional group at the *para* position of the phenyl ring of the phenyl piperazinyl methyl group was involved in electrophilic interaction with Lys 166. Pro 140 was the major contributor of hydrophobic interaction for the aromatic indole nucleus. The aliphatic chains of Glu 89 and Gln 91 also interacted hydrophobically with the indole moiety. The aromatic ring of Tyr 181 and the aliphatic chain of Gln 182 were involved in steric interaction with the terminal methoxy group. The chlorophenyl ring was well accommodated in the pocket bordered by the hydrophobic amino acid residues Trp 88, Val 90 and Lys 166. These residues also form the binding pocket for standard NNRTIs [25]. In summary, the results of the GOLD docking results supported our designed and synthesized compounds. Further structural optimization of **B21** for enhanced anti-HIV activity will be based on these facts highlighted by this docking simulation.

4.2.2. MTB ICL docking

With the intention of investigating the binding manner of our designed analogues, a docking simulation was performed using Autodock 4.0. Compound **B30** was docked into the active site pocket of MTB ICL, the coordinates of which were taken from the crystal structure of ICL/Pyruvate complex. Eleven residues were present in

the active site pocket, which was defined by a distance of 11.0 Å from the centre of the active site. The docking analysis afforded a view (Fig. 3B and D) of the hydrogen bonding interactions between the ligand and the active site residues of the protein. The hydroxyl of the quinoliny carboxylate was engaged in hydrogen bonding interactions with Tyr 89, Ser 91, Gly 92 and Trp 93. The carbonyl oxygen of the quinoliny carboxylate was hydrogen bonded to Tyr 89. The carbonyl oxygen at C₄ of quinoline moiety was involved in hydrogen bonding with the nitrogen of the peptide backbone of Trp 93. The N₄ of piperazine was found to be hydrogen bonded to imidazolyl nitrogen of His 193. The fluoroquinoline moiety was nestled in the hydrophobic pocket formed by the aromatic Trp 93, Leu 194, Thr 347 and Leu 348. Specifically, Trp 93 by virtue of its π -cloud provided favorable aromatic interaction with the quinoliny moiety. The cyclopropyl moiety attached to the N-1 of quinoline was located in the pocket formed by Trp 283, Pro 316, Thr 347 and Leu 348. The fluorine atom at C₆ of quinoline was hydrogen bonded to Ser191 and it also possessed electrophilic interactions with Trp 93, Leu 194 and Leu 348. The carboxylate moiety at C₃ was also hydrogen bonded to the metal atom, Mg⁺⁺ ion of the protein. These residues also have significant implications in binding prototype ICL inhibitors viz. 3-NP and 3-bromo pyruvate [6].

5. Conclusion

B21 was found to be the most potent in inhibiting the replication of HIV-1 cells. It also inhibited HIV-1 RT to moderate extent and even had moderate inhibitory profile against MTB ICL. By taking into account the facts highlighted by the CoMFA-COMSIA studies and the docking analyses **B21** can be further modified structurally for optimal activity against both HIV and TB infection; thereby proving efficacious against HIV-TB co-infection.

6. Experimental

6.1. Chemistry

Melting points were determined on an electro thermal melting point apparatus (Buchi BM530) in open capillary tubes and are uncorrected. All the synthetic steps were monitored till completion using thin layer chromatography. IR spectra for the compounds were recorded using Jasco IR Report 100 (KBr pellet) Spectrophotometer. ^1H NMR spectra were recorded on a JEOL Fx 400 MHz NMR spectrometer using DMSO- d_6 as solvent. Chemical shifts are expressed in δ (ppm) relative to tetramethylsilane. Elemental analyses (C, H, and N) were performed on Perkin Elmer model 240C analyzer and the data were within $\pm 0.4\%$ of the theoretical values.

6.1.1. General method for the synthesis of thiosemicarbazides (A3, B3)

To a solution of N-hydroxylamine(**A1**)/N-methoxylamine(**B1**) (0.01 mol) in absolute ethanol (20 mL) was added potassium hydroxide (0.01 mol) and carbon disulphide (0.75 mL), and the mixture was stirred at 0–5 °C for 1 h to form the corresponding potassium salt of dithiocarbamates (**A2**, **B2**). To the stirred mixture of dithiocarbamate salts was added hydrazine hydrate (0.01 mol) and the stirring was continued at 80 °C for 1 h and on adding upon crushed ice the corresponding thiosemicarbazide was obtained which is converted to hydrochloride salts (**A3**, **B3**). **A3**: Yield: 6.96%; M.P: 258–260 °C Anal[calculated/found]. C, 11.21/11.19; H, 4.70/4.68; N, 39.22/39.10 $\text{CH}_5\text{N}_3\text{OS}$; **B3**: Yield: 50.96%; M.P: 100–102 °C Anal[calculated/found]. C, 19.83/19.80; H, 5.82/5.87; N, 34.68/34.61 $\text{C}_2\text{H}_7\text{N}_3\text{OS}$.

6.1.2. General method for the synthesis of thiosemicarbazones (A4–6, B4–6)

To a hot dispersion of **A3**/**B3** (0.001M) in ethanol was added an equimolar aqueous solution of sodium acetate. To this solution further an equimolar ethanolic solution of various 5-substituted isatin was added and the mixture was stirred while being heated on a hot plate for 4–15 min, with immediate precipitation of a bulky solid. The resultant precipitate was filtered off and dried. The product was recrystallized from 95% ethanol.

6.1.2.1. (3Z)-5-Chloro-1H-indole-2,3-dione 3-(N-hydroxy thiosemicarbazone) (A4). %Yield: 62.96; M.P: 210 °C (d); ^1H NMR (DMSO- d_6 , 400 MHz) δ 7.34 (d, 1H at C₆ of indolyl), 7.42 (d, 1H at C₇ of indolyl), 7.61 (s, 1H, NH of indolyl), 7.96 (s, 1H at C₄ of indolyl), 8.52 (s, 1H, hydrazino), 9.47 (d, 1H, thioamido), 10.51 (d, 1H, hydroxyl); ^{13}C NMR (DMSO- d_6 , 400 MHz) δ 115.73 (C_{4a} of indolyl), 117.17 (C₇ of indolyl), 126.97 (C₄ of indolyl), 127.36 (C₅ of indolyl), 132.14 (C₆ of indolyl), 133.18 (C₇ of indolyl), 139.86 (C_{7a} of indolyl), 152.48 (C of carbothioamido), 154.06 (C₂ of indolyl); Anal[calculated/found]. C, 39.93/39.97; H, 2.61/2.57; N, 20.70/20.66 $\text{C}_9\text{H}_7\text{ClN}_4\text{O}_2\text{S}$.

6.1.2.2. (3Z)-5-Fluoro-1H-indole-2,3-dione 3-(N-hydroxy thiosemicarbazone) (A5). %Yield: 56.57; M.P: 223–225 °C; IR (KBr, cm^{-1}) 1740 (amide stretch), 1625 (C=N stretch), 3010 (Aromatic C–H stretch),

stretch), 3300 (amide NH stretch); ^1H NMR (DMSO- d_6 , 400 MHz) δ 7.02 (d, 1H at C₆ of indolyl), 7.37 (d, 1H at C₇ of indolyl), 7.61 (s, 1H at N1 of indolyl), 7.79 (s, 1H at C₄ of indolyl), 8.52 (s, 1H, hydrazino), 9.47 (d, 1H, thioamido), 10.51 (d, 1H, hydroxyl); ^{13}C NMR (DMSO- d_6 , 400 MHz) δ 111.74 (C₆ of indolyl), 115.22 (C₄ of indolyl), 116.74 (C₇ of indolyl), 125.51 (C_{4a} of indolyl), 131.03 (C₃ of indolyl), 138.1 (C_{7a} of indolyl), 151.53 (C₅ of indolyl), 152.48 (C of carbothioamido), 154.06 (C₂ of indolyl); Anal[calculated/found]. C, 42.52/42.56; H, 2.78/2.72; N, 22.04/22.08 $\text{C}_9\text{H}_7\text{FN}_4\text{O}_2\text{S}$.

6.1.2.3. (3Z)-5-Methyl-1H-indole-2,3-dione 3-(N-hydroxy thiosemicarbazone) (A6). %Yield: 63.63; M.P: 197–200 °C; ^1H NMR (DMSO- d_6 , 400 MHz) δ 2.31 (s, 3H, CH₃ at C5 of indolyl), 6.75 (d, 1H at C₆ of indolyl), 7.03 (d, 1H at C₇ of indolyl), 7.43 (s, 1H at C₄ of indolyl), 7.57 (s, 1H at N₁ of indolyl), 8.51 (s, 1H, hydrazino), 9.48 (d, 1H, thioamido), 10.52 (d, 1H, hydroxyl); ^{13}C NMR (DMSO- d_6 , 400 MHz) δ 20.58 (CH₃), 113.37 (C₇ of indolyl), 126.05 (C_{4a} of indolyl), 127.6 (C₆ of indolyl), 129.33 (C₅ of indolyl), 129.78 (C₄ of indolyl), 133.13 (C₃ of indolyl), 140 (C_{7a} of indolyl), 152.48 (C of carbothioamido), 154.06 (C₂ of indolyl); Anal[calculated/found]. C, 47.99/47.95; H, 4.03/4.07; N, 22.39/22.35; $\text{C}_{10}\text{H}_{10}\text{N}_4\text{O}_2\text{S}$.

6.1.2.4. (3Z)-5-Chloro-1H-indole-2,3-dione 3-(N-methoxy thiosemicarbazone) B4. %Yield: 35.63; M.P: 223–225 °C; ^1H NMR (DMSO- d_6 , 400 MHz) δ 9.2 (s, 1H, thioamido), 8.9 (s, 1H, hydrazino), 7.92 (s, 1H at C₄ of indolyl), 7.78 (d, 1H at C₆ of indolyl), 7.61 (s, 1H at N₁ of indolyl), 7.43 (d, 1H at C₇ of indolyl), 3.41 (s, 3H, CH₃ of methoxy); ^{13}C NMR (DMSO- d_6 , 400 MHz) δ 65.37 (C of methoxy thiosemicarbazone), 117.17 (C₇ of indolyl), 118.7 (C_{4a} of indolyl), 126.97 (C₄ of indolyl), 127.36 (C₅ of indolyl), 132.14 (C₆ of indolyl), 133.18 (C₃ of indolyl), 139.86 (C_{7a} of indolyl), 154.06 (C₂ of indolyl), 158.93 (C of carbothioamido); Anal[calculated/found]. C, 42.18/42.22; H, 3.19/3.23; N, 19.68/19.65 $\text{C}_{10}\text{H}_9\text{ClN}_4\text{O}_2\text{S}$.

6.1.2.5. (3Z)-5-Fluoro-1H-indole-2,3-dione 3-(N-methoxy thiosemicarbazone) B5. %Yield: 27.54; M.P: 214–216 °C; ^1H NMR (DMSO- d_6 , 400 MHz) δ 9.25 (s, 1H, thioamido), 8.94 (s, 1H, hydrazino), 7.91 (s, 1H at C₄ of indolyl), 7.81 (d, 1H at C₆ of indolyl), 7.63 (s, 1H at N₁ of indolyl), 7.46 (d, 1H at C₇ of indolyl), 3.45 (s, 3H, CH₃ of methoxy); ^{13}C NMR (DMSO- d_6 , 400 MHz) δ 65.37 (C of methoxy thiosemicarbazone), 111.74 (C₆ of indolyl), 115.22 (C₄ of indolyl), 116.74 (C₇ of indolyl), 125.59 (C_{4a} of indolyl), 131.03 (C₃ of indolyl), 138.1 (C_{7a} of indolyl), 151.53 (C₅ of indolyl), 154.06 (C₂ of indolyl), 158.93 (C of carbothioamido); Anal[calculated/found]. C, 44.77/44.59; H, 3.38/3.36; N, 20.88/20.96 $\text{C}_{10}\text{H}_9\text{FN}_4\text{O}_2\text{S}$.

6.1.2.6. (3Z)-5-Methyl-1H-indole-2,3-dione 3-(N-methoxy thiosemicarbazone) B6. %Yield: 34.72; M.P: 186–188 °C; IR (KBr, cm^{-1}) 1740 (amide stretch), 1625 (C=N stretch), 3010 (Aromatic C–H stretch), 3300 (amide NH stretch); ^1H NMR (DMSO- d_6 , 400 MHz) δ 9.17 (s, 1H, thioamido), 8.87 (s, 1H, hydrazino), 7.89 (s, 1H at C₄ of indolyl), 7.63 (s, 1H at N₁ of indolyl), 7.16 (d, 1H at C₇ of indolyl), 6.92 (d, 1H at C₆ of indolyl), 3.53 (s, 3H, CH₃ of methoxy), 2.57 (s, 3H, methoxy); ^{13}C NMR (DMSO- d_6 , 400 MHz) δ 20.58 (CH₃), 65.37 (C of methoxy thiosemicarbazone), 113.37 (C₇ of indolyl), 126.13 (C_{4a} of indolyl), 127.6 (C₆ of indolyl), 129.33 (C₅ of indolyl), 129.78 (C₄ of indolyl), 133.13 (C₃ of indolyl), 140 (C_{7a} of indolyl), 154.06 (C₂ of indolyl), 158.93 (C of carbothioamido); Anal[calculated/found]. C, 49.99/49.79; H, 4.58/4.54; N, 21.20/21.28; $\text{C}_{11}\text{H}_{12}\text{N}_4\text{O}_2\text{S}$.

6.1.3. General method for the synthesis of N-mannich bases of 5-substituted-1H-indole-2,3-dione 3-(N-hydroxy/methoxy-thiosemicarbazones) (A7–36, B7–36)

To an ethanolic solution of N-hydroxy/methoxy thiosemicarbazones (0.00045 M) was added an equimolar amount of

various secondary amines, dissolved in ethanol or dimethyl sulfoxide. To this mixture, an equimolar amount of 30% formaldehyde solution was then added and this mixture was then irradiated with microwave of 455 W in a scientific microwave reactor accompanied by continuous stirring, which was attained by means of a magnetic plate, placed underneath the floor of the magnetic cavity and a Teflon-coated magnetic bead in the reaction vessel, for approximately three to 15 min. At the end of the reaction period, the product precipitated out, which was filtered off and dried. The resultant precipitate was recrystallized from ethanol.

6.1.3.1. 2-{[5-chloro-1-[(dimethylamino)methyl]-2-oxo-1,2-dihydro-3H-indol-3-yliden]-N-hydroxyhydrazine-1-carbothioamide (A7)}. % Yield: 97.05; M.P: 102–104 °C; IR (cm⁻¹; KBr) 3030, 2850, 1730, 1620, 1210, 850; ¹H NMR (DMSO-*d*₆, 400 MHz) δ 2.07 (s, 6H, dimethylamine), 5.92 (s, 2H, -NCH₂N-), 6.61 (d, 1H, indolyl C₇), 6.92 (d, 1H, indolyl C₆), 7.35 (s, 1H, indolyl C₄) 8.51 (s, 1H, hydrazine), 9.48 (d, 1H, thioamido), 10.52 (d, 1H, hydroxyl); ¹³C NMR (DMSO-*d*₆, 400 MHz) δ 42.9 (2C, -N(CH₃)₂), 66.33 (-CH₂), 118 (C₇ of indolyl), 124.88 (C₄ of indolyl), 126.87 (C₅ of indolyl), 127.36 (C_{4a} of indolyl), 130.12 (C₆ of indolyl), 136.12 (C₃ of indolyl), 148.65 (C_{7a} of indolyl), 152.48 (C of carbothioamido), 155.39 (C₂ of indolyl); Anal[calculated/found]. C, 43.97/43.79; H, 4.30/4.26; N, 21.37/21.35; C₁₂H₁₄ClN₅O₂S.

6.1.3.2. 2-{[1-[(Dimethylamino)methyl]-5-methyl-2-oxo-1,2-dihydro-3H-indol-3-yliden]-N-hydroxyhydrazine-1-carbothioamide (A9)}. % Yield: 95.85; M.P: 110 °C; ¹H NMR (DMSO-*d*₆, 400 MHz) δ 2.13 (s, 6H, dimethylamino), 2.65 (s, 3H, CH₃ at C₅ of indolyl), 5.92 (s, 2H, -NCH₂N-), 7.11 (d, 1H, C₇ of indolyl), 7.23 (d, 1H, C₆ of indolyl), 7.47 (s, 1H, C₄ of indolyl), 8.52 (s, 1H, hydrazine), 9.48 (d, 1H, thioamido), 10.51 (d, 1H, hydroxyl); ¹³C NMR (DMSO-*d*₆, 400 MHz) δ 20.58 (CH₃ at C₅ of indolyl), 42.9 (2C, -N(CH₃)₂), 66.33 (-CH₂), 115.45 (C₇ of indolyl), 124.39 (C₅ of indolyl), 126.14 (C₆ of indolyl), 128.92 (C_{4a} of indolyl), 129.42 (C₄ of indolyl), 136.07 (C₃ of indolyl), 149.99 (C_{7a} of indolyl), 152.48 (C of carbothioamido), 155.39 (C₂ of indolyl); Anal[calculated/found]. C, 50.80/50.66; H, 5.57/5.53; N, 22.78/22.85; C₁₃H₁₇N₅O₂S.

6.1.3.3. 2-{[1-[(Diethylamino)methyl]-5-fluoro-2-oxo-1,2-dihydro-3H-indol-3-yliden]-N-hydroxyhydrazine-1-carbothioamide (A11)}. %Yield: 79.90; M.P: 80–82 °C; IR (cm⁻¹; KBr) 3040, 2855, 1735, 1621, 1215, 843; ¹H NMR (DMSO-*d*₆, 400 MHz) δ 1.03 (t, 6H, (CH₂CH₃)₂), 2.59 (q, 4H, (CH₂CH₃)₂), 5.94 (s, 2H, -NCH₂N-), 6.65 (d, 1H, C₇ of indolyl), 7.22 (d, 1H, C₆ of indolyl), 7.83 (s, 1H, C₄ of indolyl), 8.52 (s, 1H, hydrazine), 9.49 (d, 1H, thioamido), 10.45 (d, 1H, hydroxyl); ¹³C NMR (DMSO-*d*₆, 400 MHz) δ 12.01 (2C of CH₃ of -N(C₂H₅)₂), 42.89 (2C of CH₂ of -N(C₂H₅)₂), 61.91 (-CH₂), 111.71 (C₆ of indolyl), 113.91 (C₄ of indolyl), 117.76 (C₇ of indolyl), 127.75 (C_{4a} of indolyl), 133.61 (C₃ of indolyl), 146.12 (C_{7a} of indolyl), 147.57 (C₅ of indolyl), 152.48 (C of carbothioamido), 155.39 (C₂ of indolyl); Anal[calculated/found]. C, 49.54/49.37; H, 5.35/5.33; N, 20.64/20.69; C₁₄H₁₈FN₅O₂S.

6.1.3.4. 2-{[1-[(Diethylamino)methyl]-5-methyl-2-oxo-1,2-dihydro-3H-indol-3-yliden]-N-hydroxyhydrazine-1-carbothioamide (A12)}. % Yield: 71.47; M.P: 114–116 °C; ¹H NMR (DMSO-*d*₆, 400 MHz) δ 1.08 (t, 6H, (CH₂CH₃)₂), 2.14 (s, 3H, CH₃) 2.53 (q, 4H, (CH₂CH₃)₂), 5.87 (s, 2H, -NCH₂N-), 6.47 (d, 1H, C₇ of indolyl), 7.19 (d, 1H, C₆ of indolyl), 7.64 (s, 1H, C₄ of indolyl), 8.51 (s, 1H, hydrazine), 9.47 (d, 1H, thioamido), 10.43 (d, 1H, hydroxyl); ¹³C NMR (DMSO-*d*₆, 400 MHz) δ 12.03 (2C of CH₃ of -N(C₂H₅)₂), 20.58 (CH₃ at C₅ of indolyl), 42.89 (2C of CH₂ of -N(C₂H₅)₂), 61.91 (-CH₂), 115.07 (C₇ of indolyl), 124.39 (C₅ of indolyl), 124.57 (C₆ of indolyl), 128.93 (C_{4a} of indolyl), 129.42 (C₄ of indolyl), 136.07 (C₃ of indolyl), 149.59 (C_{7a} of indolyl), 152.48 (C of carbothioamido), 155.39 (C₂ of indolyl); Anal

[calculated/found]. C, 53.71/53.53; H, 6.31/6.34; N, 20.88/20.95; C₁₅H₂₁N₅O₂S.

6.1.3.5. 2-[5-chloro-1-(1,4-oxazinan-4-ylmethyl)-2-oxo-1,2-dihydro-3H-indol-3-yliden]-N-hydroxyhydrazine-1-carbothioamide (A13)}. % Yield: 56.43; M.P: 46–48 °C; IR (cm⁻¹; KBr) 3020, 2847, 1725, 1615, 1220, 852; ¹H NMR (DMSO-*d*₆, 400 MHz) δ 2.64 (t, 4H, C₃, C₅ of morpholinyl), 3.55 (t, 4H, C₂, C₆ of morpholinyl), 5.67 (s, 2H, -NCH₂N-), 6.91 (d, 1H, C₇ of indolyl), 7.41 (d, 1H, C₆ of indolyl), 8.04 (s, 1H, C₄ of indolyl), 8.49 (s, 1H, hydrazine), 9.46 (d, 1H, thioamido), 10.51 (d, 1H, hydroxyl); ¹³C NMR (DMSO-*d*₆, 400 MHz) δ 56.69 (2C, C₃, C₅ of morpholinyl), 58.8 (2C, C₂, C₆ of morpholinyl), 62.14 (-CH₂), 118.23 (C₇ of indolyl), 124.88 (C₄ of indolyl), 126.87 (C₅ of indolyl), 127.58 (C_{4a} of indolyl), 130.12 (C₆ of indolyl), 136.12 (C₃ of indolyl), 146.91 (C_{7a} of indolyl), 152.48 (C of carbothioamido), 155.39 (C₂ of indolyl); Anal[calculated/found]. C, 45.47/45.65; H, 4.36/4.35; N, 18.94/18.88C₁₄H₁₆ClN₅O₃S.

6.1.3.6. 2-(5-Fluoro-2-oxo-1-[[4-phenyltetrahydropyrazin-1(2H)-yl]methyl]-1,2-dihydro-3H-indol-3-yliden)-N-hydroxyhydrazine-1-carbothioamide (A17)}. %Yield: 86.09; M.P: 78–80 °C; ¹H NMR (DMSO-*d*₆, 400 MHz) δ 3.11 (t, 4H, C₂, C₆ of piperazinyl), 3.18 (t, 4H, C₃, C₅ of piperazinyl), 6.50 (d, 1H, C₇ of indolyl), 6.63 (d, 2H, C₂, C₆ of phenyl), 6.81 (m, 1H, C₄ of phenyl), 7.25 (d, 2H, C₃, C₅ of phenyl), 7.30 (d, 1H, C₆ of indolyl), 7.63 (s, 1H, C₄ of indolyl), 8.51 (s, 1H, hydrazine), 9.47 (d, 1H, thioamido), 10.52 (d, 1H, hydroxyl); ¹³C NMR (DMSO-*d*₆, 400 MHz) δ 48.17 (2C, C₃, C₅ of piperazinyl), 51.73 (2C, C₂, C₆ of piperazinyl), 62.25 (-CH₂), 113.91 (C₄ of indolyl), 115.07 (C₆ of indolyl), 116.35 (2C, C₂, C₆ of phenyl), 117.69 (C₇ of indolyl), 120.3 (C₄ of phenyl), 128.19 (C_{4a} of indolyl), 129.1 (2C, C₃, C₅ of phenyl), 133.61 (C₃ of indolyl), 145.62 (C_{7a} of indolyl), 147.57 (C₅ of indolyl), 150.73 (C₁ of phenyl), 152.48 (C of carbothioamido), 155.39 (C₂ of indolyl); Anal[calculated/found]. C, 56.06/55.84; H, 4.94/4.96; N, 19.61/19.57C₂₀H₂₁FN₆O₂S.

6.1.3.7. N-Hydroxy-2-(5-methyl-2-oxo-1-[[4-phenyl-tetrahydropyrazin-1(2H)-yl]methyl]-1,2-dihydro-3H-indol-3-yliden)hydrazine-1-carbothioamide (A18)}. %Yield: 79.93; M.P: 68–70 °C; IR (cm⁻¹; KBr) 3030, 2850, 1731, 1622, 1210, 845; ¹H NMR (DMSO-*d*₆, 400 MHz) δ 2.26 (s, 3H, CH₃), 3.15 (t, 4H, C₂, C₆ of piperazinyl), 3.17 (t, 4H, C₃, C₅ of piperazinyl), 5.13 (s, 2H, -NCH₂N-), 6.41 (d, 2H, C₂, C₆ of phenyl), 6.71 (d, 1H, C₇ of indolyl), 6.77 (m, 1H, C₄ of phenyl), 7.11 (d, 1H, C₆ of indolyl), 7.35 (d, 2H, C₃, C₅ of phenyl), 7.76 (s, 1H, C₄ of indolyl), 8.52 (s, 1H, hydrazine), 9.47 (d, 1H, thioamido), 10.53 (d, 1H, hydroxyl); ¹³C NMR (DMSO-*d*₆, 400 MHz) δ 20.58 (CH₃ at C₅ of indolyl), 48.17 (2C, C₃, C₅ of piperazinyl), 51.73 (2C, C₂, C₆ of piperazinyl), 62.25 (-CH₂), 115.89 (C₇ of indolyl), 116.35 (2C, C₂, C₆ of phenyl), 120.3 (C₄ of phenyl), 124.39 (C₅ of indolyl), 126.14 (C₆ of indolyl), 129.1 (2C, C₃, C₅ of phenyl), 129.37 (C_{4a} of indolyl), 129.42 (C₄ of indolyl), 136.07 (C₃ of indolyl), 148.71 (C_{7a} of indolyl), 150.73 (C₁ of phenyl), 152.48 (C of carbothioamido), 155.39 (C₂ of indolyl); Anal[calculated/found]. C, 59.51/59.41; H, 5.70/5.70; N, 19.80/19.80; C₂₁H₂₄N₆O₂S.

6.1.3.8. 2-(1-[[4-(4-Chlorophenyl)tetrahydropyrazin-1(2H)-yl]methyl]-5-methyl-2-oxo-1,2-dihydro-3H-indol-3-yliden)-N-hydroxyhydrazine-1-carbothioamide (A21)}. %Yield: 76.34; M.P: 178–182 °C; IR (cm⁻¹; KBr) 3015, 2853, 1727, 1625, 1220, 853; ¹H NMR (DMSO-*d*₆, 400 MHz) δ 2.56 (s, 3H, CH₃), 3.14 (t, 4H, C₂, C₆ of piperazinyl), 3.18 (t, 4H, C₃, C₅ of piperazinyl), 5.73 (s, 2H, -NCH₂N-), 6.34 (d, 2H, C₂, C₆ of phenyl), 6.63 (d, 1H, C₇ of indolyl), 6.81 (d, 2H, C₃, C₅ of phenyl), 7.54 (s, 1H, C₄ of indolyl), 8.53 (s, 1H, hydrazine), 9.47 (d, 1H, thioamido), 10.53 (d, 1H, hydroxyl); ¹³C NMR (DMSO-*d*₆, 400 MHz) δ 20.58 (CH₃ at C₅ of indolyl), 48.17 (2C, C₃, C₅ of piperazinyl), 51.73 (2C, C₂, C₆ of piperazinyl), 62.25 (-CH₂),

115.89 (C₇ of indolyl), 124.39 (C₅ of indolyl), 124.84 (2C, C₂, C₆ of Phenyl), 126.14 (C₆ of indolyl), 127.93 (2C, C₃, C₅ of Phenyl), 129.37 (C_{4a} of Indolyl), 129.42 (C₄ of indolyl), 129.95 (C₄ of Phenyl), 136.07 (C₃ of indolyl), 146.74 (C₁ of Phenyl), 148.71 (C_{7a} of Indolyl), 152.48 (C of carbothioamido), 155.39 (C₂ of indolyl); Anal[calculated/found]. C, 54.96/55.16; H, 5.05/5.03; N, 18.31/18.27C₂₁H₂₃ClN₆O₂S.

6.1.3.9. 2-(5-Chloro-1-[[4-[4-(methyloxy)phenyl]tetrahydropyrazin-1(2H)-yl]methyl]-2-oxo-1,2-dihydro-3H-indol-3-yliden)-N-hydroxyhydrazine-1-carbothioamide (**A22**). %Yield: 58.32; M.P: 140 °C; IR (cm⁻¹; KBr) 3025, 2845, 1720, 1622, 1230, 848; ¹H NMR (DMSO-*d*₆, 400 MHz) δ 3.15 (t, 4H, C₂, C₆ of piperazinyl), 3.21 (t, 4H, C₃, C₅ of piperazinyl), 3.77 (s, 3H, 4-methoxyphenyl) 5.16 (s, 2H, -NCH₂N-), 6.16(d, 2H, C₂, C₆ of phenyl), 7.43 (d, 1H, C₇ of indolyl), 6.62 (d, 2H, C₃, C₅ of phenyl), 6.89 (d, 1H, C₆ of indolyl), 8.14 (s, 1H, C₄ of indolyl), 8.53 (s, 1H, hydrazino), 9.46 (d, 1H, thioamido), 10.51 (d, 1H, hydroxyl); ¹³C NMR (DMSO-*d*₆, 400 MHz) δ 48.17 (C₃, C₅ of piperazinyl), 51.73 (2C, C₂, C₆ of piperazinyl), 55.2 (C of methoxy phenyl), 62.25 (-CH₂-), 112.82 (2C, C₃, C₅ of Phenyl), 118.45 (C₇ of indolyl), 124.44 (2C, C₂, C₆ of Phenyl), 124.88 (C₄ of indolyl), 126.87 (C₅ of indolyl), 127.8 (C_{4a} of indolyl), 130.12 (C₆ of indolyl), 136.12 (C₃ of indolyl), 142.19 (C₁ of Phenyl), 146.83 (C_{7a} of indolyl), 152.48 (C of carbothioamido), 155.39 (C₂ of indolyl), 157.24 (C₄ of Phenyl); Anal[calculated/found]. C, 53.10/52.91; H, 4.88/4.89; N, 17.69/17.63C₂₁H₂₃ClN₆O₃S.

6.1.3.10. N-Hydroxy-2-(5-methyl-1-[[4-[4-(methyloxy)phenyl]tetrahydropyrazin-1(2H)-yl]methyl]-2-oxo-1,2-dihydro-3H-indol-3-yliden)hydrazine-1-carbothioamide (**A24**). %Yield: 88.66; M.P: 216–218 °C; ¹H NMR (DMSO-*d*₆, 400 MHz) δ 2.83 (s, 3H, CH₃), 3.23 (t, 4H, C₂, C₆ of piperazinyl), 3.34 (t, 4H, C₃, C₅ of piperazinyl), 3.65 (s, 3H, 4-methoxyphenyl) 4.97 (s, 2H, -NCH₂N-), 6.23(d, 2H, C₂, C₆ of phenyl), 7.34 (d, 1H, C₇ of indolyl), 6.81 (d, 2H, C₃, C₅ of phenyl), 6.89 (d, 1H, C₆ of indolyl), 7.83 (s, 1H, C₄ of indolyl), 8.51 (s, 1H, hydrazine), 9.45 (d, 1H, thioamido), 10.53 (d, 1H, hydroxyl); ¹³C NMR (DMSO-*d*₆, 400 MHz) δ 20.58 (CH₃), 48.17 (2C, C₃, C₅ of Piperazinyl), 51.73 (2C, C₂, C₆ of Piperazinyl), 55.2 (CH₃ of 4-methoxy phenyl), 62.25 (-CH₂-), 112.82 (2C, C₃, C₅ of phenyl), 115.89 (C₇ of indolyl), 124.39 (C₅ of indolyl), 124.44 (2C, C₂, C₆ of indolyl), 126.14 (C₆ of indolyl), 129.37 (C_{4a} of indolyl), 129.42 (C₄ of indolyl), 136.07 (C₃ of indolyl), 142.19 (C₁ of phenyl), 148.71 (C_{7a} of indolyl), 152.48 (C of carbothioamido), 155.39 (C₂ of indolyl), 157.24 (C₄ of Phenyl); Anal [calculated/found]. C, 58.13/57.92; H, 5.77/5.79; N, 18.49/18.54; C₂₂H₂₆N₆O₃S.

6.1.3.11. 1-Ethyl-6-fluoro-7-[4-(3-((Z)-2-[(hydroxyamino)carbothiyl]hydrazono)-5-methyl-2-oxo-2,3-dihydro-1H-indol-1-yl)]hexahydropyrazin-1-yl]-4-oxo-1,4-dihydroquinoline-3-carboxylic acid (**A27**). %Yield: 47.33; M.P: 180–182 °C (d); ¹H NMR (DMSO-*d*₆, 400 MHz) δ 1.21 (t, 3H, CH₃ of C₂H₅), 2.37 (s, 3H, methyl at C₅ of indole), 3.11 (t, 4H, C₂, C₆ of piperazinyl), 3.15 (t, 4H, C₃, C₅ of piperazinyl), 4.26 (q, 2H, CH₂ of C₂H₅), 5.16 (s, 2H, methylene CH₂), 6.21 (s, 1H at C₈ of quinoliny), 6.73 (d, 1H at C₇ of indolyl), 7.14 (d, 1H at C₆ of indolyl), 7.25 (s, 1H at C₅ of quinoliny), 7.29 (s, 1H at C₄ of indolyl), 7.35 (s, 1H at C₂ of quinoliny), 8.52 (s, 1H, hydrazino), 9.47 (d, 1H, thioamido), 10.51 (d, 1H, hydroxyl); ¹³C NMR (DMSO-*d*₆, 400 MHz) δ 14.4 (CH₃ of C₂H₅ at N₁ of quinoliny), 20.58 (CH₃ at C₅ of indolyl), 49.01 (CH₂ of C₂H₅ at N₁ of quinoliny), 50.02 (2C, C₃, C₅ of piperazinyl), 51.73 (2C, C₂, C₆ of piperazinyl), 62.25 (-CH₂-), 106.84 (C₈ of quinoliny), 107.2 (C₃ of quinoliny), 111.2 (C₅ of quinoliny), 115.89 (C₇ of indolyl), 119.8 (C_{4a} of quinoliny), 124.39 (C₅ of indolyl), 126.14 (C₆ of indolyl), 129.37 (C_{4a} of indolyl), 129.42 (C₄ of indolyl), 136.07 (C₃ of indolyl), 136.9 (C_{8a} of quinoliny), 143.37 (C₇ of quinoliny), 148.4 (C₂ of quinoliny), 148.71 (C_{7a} of indolyl), 152.48 (C of carbothioamido), 152.83 (C₆ of quinoliny), 155.39 (C₂ of indolyl), 165.6 (C of COOH),

175.8 (C₄ of quinoliny); Anal[calculated/found]. C, 55.76/55.57; H, 4.85/4.86; N, 16.86/16.89C₂₇H₂₈FN₇O₅S.

6.1.3.12. 1-Cyclopropyl-6-fluoro-7-[4-(5-fluoro-3-((Z)-2-[(hydroxyamino)carbothiyl]hydrazono)-2-oxo-2,3-dihydro-1H-indol-1-yl)]hexahydropyrazin-1-yl]-4-oxo-1,4-dihydroquinoline-3-carboxylic acid (**A29**). %Yield: 90.62; M.P: 230(d)°C; IR (cm⁻¹; KBr) 3455, 3040, 2835, 1728, 1615, 1225, 846; ¹H NMR (DMSO-*d*₆, 400 MHz) δ 0.39 (m, 4H, CH₂ of cyclopropyl), 2.51 (t, 1H, CH of cyclopropyl), 3.11 (t, 4H, C₂, C₆ of piperazinyl), 3.17 (t, 4H, C₃, C₅ of piperazinyl), 5.09 (s, 2H, methylene), 6.41 (s, 1H at C₈ of quinoliny), 6.61 (d, 1H at C₇ of indolyl), 6.97 (s, 1H at C₅ of quinoliny), 7.18 (d, 1H at C₆ of indolyl), 7.51 (s, 1H at C₂ of quinoliny), 7.73 (s, 1H at C₄ of indolyl), 8.53 (s, 1H, hydrazino), 9.46 (d, 1H, thioamido), 10.51 (d, 1H, hydroxyl); ¹³C NMR (DMSO-*d*₆, 400 MHz) δ 7.7 (2C, CH₂ of cyclopropyl), 30.6 (CH of cyclopropyl), 50.02 (2C, C₃, C₅ of piperazinyl), 51.73 (2C, C₂, C₆ of piperazinyl), 62.25 (-CH₂-), 99.43 (C₈ of quinoliny), 103.6 (C₅ of quinoliny), 107.6 (C₃ of quinoliny), 112.3 (C_{5a} of quinoliny), 113.91 (C₄ of indolyl), 115.07 (C₆ of indolyl), 117.69 (C₇ of indolyl), 128.19 (C_{4a} of indolyl), 133.03 (C_{8a} of indolyl), 133.61 (C₃ of indolyl), 139.76 (C₇ of quinoliny), 140.9 (C₂ of quinoliny), 145.62 (C_{7a} of indolyl), 147.57 (C₅ of indolyl), 148.43 (C₆ of quinoliny), 152.48 (C of carbothioamido), 155.39 (C₂ of indolyl), 161.9 (C of COOH), 177.5 (C₄ of quinoliny); Anal[calculated/found]. C, 54.27/54.08; H, 4.22/4.23; N, 16.41/16.35C₂₇H₂₅F₂N₇O₅S.

6.1.3.13. 7-[4-(5-chloro-3-((Z)-2-[(hydroxyamino)carbothiyl]hydrazono)-2-oxo-2,3-dihydro-1H-indol-1-yl)]-3-methylhexahydropyrazin-1-yl]-1-ethyl-6,8-difluoro-4-oxo-1,4-dihydroquinoline-3-carboxylic acid (**A31**). %Yield: 88.59; M.P: 226–228 °C; IR (cm⁻¹; KBr) 3500, 3020, 2841, 1725, 1621, 1217, 845; ¹H NMR (DMSO-*d*₆, 400 MHz) δ 0.94 (d, 3H, CH₃ at C₃ of piperazinyl), 1.18 (t, 3H of CH₃ of C₂H₅), 2.85 (d, 2H at C₂ of piperazinyl), 3.14 (t, 2H at C₆ of piperazinyl), 3.21 (m, 1H at C₃ of piperazinyl), 3.57 (t, 2H at C₅ of piperazinyl), 4.32 (q, 2H of C₂H₅), 5.13 (s, 2H of methylene), 6.91 (d, 1H at C₇ of indolyl), 7.13 (s, 1H at C₅ of quinoliny), 7.41 (d, 1H at C₆ of indolyl), 7.52 (s, 1H at C₂ of quinoliny), 7.95 (s, 1H at C₄ of indolyl), 8.52 (s, 1H, hydrazino), 9.47 (d, 1H, thioamido), 10.51 (d, 1H, hydroxyl); ¹³C NMR (DMSO-*d*₆, 400 MHz) δ 15.7 (CH₃ of C₂H₅ at N₁ of quinoliny), 18.12 (CH₃ at C₃ of piperazinyl), 46.41 (CH₂ of C₂H₅ at N₁ of quinoliny), 51.26 (C₄ of quinoliny), 52.38 (C₆ of piperazinyl), 52.88 (C₅ of piperazinyl), 57.64 (C₃ of piperazinyl), 60.04 (-CH₂-), 62.35 (C₂ of piperazinyl), 103.89 (C₃ of quinoliny), 108.28 (C₅ of quinoliny), 112.89 (C₇ of quinoliny), 118.45 (C₇ of indolyl), 119.87 (C_{4a} of quinoliny), 124.88 (C₄ of indolyl), 126.87 (C₅ of indolyl), 127.8 (C_{4a} of indolyl), 130.12 (C₆ of indolyl), 130.85 (C_{8a} of quinoliny), 136.12 (C₃ of indolyl), 139.48 (C₈ of quinoliny), 142.58 (C₆ of quinoliny), 145.61 (C₂ of quinoliny), 146.49 (C_{7a} of indolyl), 152.48 (C of carbothioamido), 155.39 (C₂ of indolyl), 169.04 (C of COOH); Anal[calculated/found]. C, 51.15/51.29; H, 4.13/4.15; N, 15.46/15.48; C₂₇H₂₆ClF₂N₇O₅S.

6.1.3.14. 1-Ethyl-6,8-difluoro-7-[4-(3-((Z)-2-[(hydroxyamino)carbothiyl]hydrazono)-5-methyl-2-oxo-2,3-dihydro-1H-indol-1-yl)]-3-methylhexahydropyrazin-1-yl]-4-oxo-1,4-dihydroquinoline-3-carboxylic acid (**A33**). %Yield: 81.22; M.P: 140–144 °C; ¹H NMR (DMSO-*d*₆, 400 MHz) δ 0.96 (d, 3H, CH₃ at C₃ of piperazinyl), 1.17 (t, 3H of CH₃ of C₂H₅), 2.41 (s, 3H, methyl at C₅ of indolyl), 2.87 (d, 2H at C₂ of piperazinyl), 3.13 (t, 2H at C₆ of piperazinyl), 3.19 (m, 1H at C₃ of piperazinyl), 3.58 (t, 2H at C₅ of piperazinyl), 4.34 (q, 2H of C₂H₅), 5.15 (s, 2H of methylene), 6.92 (d, 1H at C₇ of indolyl), 7.15 (s, 1H at C₅ of quinoliny), 7.43 (d, 1H at C₆ of indolyl), 7.51 (s, 1H at C₂ of quinoliny), 7.93 (s, 1H at C₄ of indolyl), 8.51 (s, 1H, hydrazino), 9.47 (d, 1H, thioamido), 10.52 (d, 1H, hydroxyl); ¹³C NMR (DMSO-*d*₆, 400 MHz) δ 15.7 (CH₃ of C₂H₅), 18.12 (CH₃ at C₃ of piperazinyl),

20.58 (CH₃ at C₅ of indolyl), 46.41 (CH₂ of C₂H₅), 51.26 (C₄ of quinolyl), 52.38 (C₆ of piperaziny), 52.88 (C₅ of piperaziny), 57.64 (C₃ of piperaziny), 60.04 (–CH₂–), 62.35 (C₂ of piperaziny), 112.89 (C₇ of quinolyl), 115.89 (C₇ of indolyl), 119.87 (C_{4a} of quinolyl), 124.39 (C₅ of indolyl), 126.14 (C₆ of indolyl), 129.37 (C_{4a} of indolyl), 129.42 (C₄ of indolyl), 136.07 (C₃ of indolyl), 139.48 (C₈ of quinolyl), 142.58 (C₆ of quinolyl), 145.61 (C₂ of quinolyl), 147.91 (C_{7a} of indolyl), 152.48 (C of carbothioamido), 155.39 (C₂ of indolyl), 169.04 (C of COOH); Anal[calculated/found]. C, 54.80/54.63; H, 4.76/4.75; N, 15.98/15.93C₂₈H₂₉F₂N₇O₅S.

6.1.3.15. 1-Cyclopropyl-6-fluoro-7-[4-(3-((Z)-2-[(hydroxyamino)carbothiyl]hydrazono)-5-methyl-2-oxo-2,3-dihydro-1H-indol-1-yl)-3-methylhexahydropyrazin-1-yl]-8-(methoxy)-4-oxo-1,4-dihydroquinoline-3-carboxylic acid (**A36**). %Yield: 77.75; M.P: 70 °C; IR (cm⁻¹; KBr) 3458, 3035, 2851, 1732, 1618, 1210, 852; NMR (DMSO-d₆, 400 MHz) δ 0.39 (m, 4H, CH₂ of cyclopropyl), 0.94 (s, 3H, CH₃ at C₃ of piperaziny), 2.41 (s, 3H, methyl at C₅ of indolyl), 2.44 (t, 1H, CH of cyclopropyl), 2.89 (d, 2H at C₂ of piperaziny), 3.14 (t, 2H at C₆ of piperaziny), 3.18 (m, 1H at C₃ of piperaziny), 3.56 (t, 2H at C₅ of piperaziny), 3.61 (s, 3H, methoxy at C₈ of quinolyl), 5.15 (s, 2H of methylene), 6.71 (d, 1H at C₇ of indolyl), 7.08 (d, 1H at C₆ of indolyl), 7.30 (s, 1H at C₄ of indolyl), 7.34 (s, 1H, C₅ of quinolyl), 7.41 (s, 1H, C₂ of quinolyl), 8.51 (s, 1H, hydrazino), 9.46 (d, 1H, thioamido), 10.53 (d, 1H, hydroxyl); ¹³C NMR (DMSO-d₆, 400 MHz) δ 7.7 (2C, CH₂ of cyclopropyl), 18.12 (CH₃ at C₃ of piperaziny), 20.58 (CH₃ at C₅ of indolyl), 31.97 (CH of cyclopropyl), 50.88 (C₆ of piperaziny), 52.88 (C₅ of piperaziny), 57.64 (C₃ of piperaziny), 57.77 (methoxy C at C₈ of quinolyl), 60.04 (–CH₂–), 60.85 (C₂ of piperaziny), 115.89 (C₇ of indolyl), 122.43 (C_{4a} of quinolyl), 122.88 (C_{8a} of quinolyl), 124.39 (C₅ of indolyl), 126.14 (C₆ of indolyl), 129.37 (C_{4a} of indolyl), 129.42 (C₄ of indolyl), 132.29 (C₇ of quinolyl), 136.07 (C₃ of indolyl), 142.76 (C₈ of quinolyl), 146.39 (C₂ of quinolyl), 147.91 (C_{7a} of indolyl), 152.48 (C of carbothioamido), 155.07 (C₆ of quinolyl), 155.39 (C₂ of indolyl), 163.68 (C of COOH), 174.28 (C₄ of quinolyl); Anal[calculated/found]. C, 56.50/56.68; H, 5.06/5.08; N, 15.38/15.34C₃₀H₃₂FN₇O₆S.

6.1.3.16. 2-{1-[(Dimethylamino)methyl]-5-fluoro-2-oxo-1,2-dihydro-3H-indol-3-yliden}-N-(methoxy)hydrazine-1-carbothioamide (**B8**). %Yield: 82.45; M.P: 56–58 °C; IR (cm⁻¹; KBr) 3020, 2847, 1726, 1615, 1205, 854; ¹H NMR (DMSO-d₆, 400 MHz) δ 2.45 (s, 6H, dimethylamino), 3.67 (s, 3H, methoxyl), 5.14 (s, 2H, –NCH₂N–), 6.63 (d, 1H, C₇ of indolyl), 7.31 (d, 1H, C₆ of indolyl), 7.82 (s, 1H, C₄ of indolyl), 8.51 (s, 1H, hydrazino), 9.48 (s, 1H, NH proton); ¹³C NMR (DMSO-d₆, 400 MHz) δ 42.9 (2C, –N(CH₃)₂), 65.37 (CH₃ of methoxy thiosemicarbazone), 66.33 (–CH₂–), 113.91 (C₄ of indolyl), 115.07 (C₆ of indolyl), 118.13 (C₇ of indolyl), 127.82 (C_{4a} of indolyl), 133.61 (C₃ of indolyl), 146.51 (C_{7a} of indolyl), 147.57 (C₅ of indolyl), 155.39 (C₂ of indolyl), 158.93 (C of carbothioamido); Anal[calculated/found]. C, 47.99/47.85; H, 4.96/4.98; N, 21.52/21.55C₁₃H₁₆FN₅O₂S.

6.1.3.17. 2-{1-[(Diethylamino)methyl]-5-fluoro-2-oxo-1,2-dihydro-3H-indol-3-yliden}-N-(methoxy)hydrazine-1-carbothioamide (**B11**). %Yield: 83.50; M.P: 98–100 °C; ¹H NMR (DMSO-d₆, 400 MHz) δ 1.17 (t, 6H, –(CH₂CH₃)₂), 2.53 (q, 4H, –(CH₂CH₃)₂), 3.59 (s, 3H, methoxyl), 5.17 (s, 2H, –NCH₂N–), 6.57 (d, 1H, C₇ of indolyl), 7.33 (d, 1H, C₆ of indolyl), 7.76 (s, 1H, C₄ of indolyl), 8.52 (s, 1H, hydrazino), 9.46 (s, 1H, NH proton); ¹³C NMR (DMSO-d₆, 400 MHz) δ 12.03 (2C, CH₃ of –N(CH₂H₅)₂), 42.89 (2C, CH₂ of –N(CH₂H₅)₂), 61.91 (–CH₂–), 65.37 (CH₃ of methoxy thiosemicarbazone), 111.71 (C₆ of indolyl), 113.91 (C₄ of indolyl), 117.76 (C₇ of indolyl), 127.83 (C_{4a} of indolyl), 133.61 (C₃ of indolyl), 146.12 (C_{7a} of indolyl), 147.57 (C₅ of indolyl), 155.39 (C₂ of indolyl), 158.93 (C of carbothioamido); Anal[calculated/found]. C, 50.98/50.89; H, 5.70/5.68; N, 19.82/19.85; C₁₅H₂₀FN₅O₂S.

6.1.3.18. 2-[5-methyl-1-(1,4-oxazinan-4-ylmethyl)-2-oxo-1,2-dihydro-3H-indol-3-yliden]-N-(methoxy)hydrazine-1-carbothioamide (**B15**). %Yield: 75.70; M.P: 86–90 °C; ¹H NMR (DMSO-d₆, 400 MHz) δ 2.43 (s, 3H, CH₃), 2.65 (t, 4H, C₃, C₅ of morpholyl), 3.56 (t, 4H, C₂, C₆ of morpholyl), 3.66 (s, 3H, methoxyl), 5.17 (s, 2H, –NCH₂N–), 6.73 (d, 1H, C₇ of indolyl), 7.13 (d, 1H, C₆ of indolyl), 7.32 (s, 1H, C₄ of indolyl), 8.51 (s, 1H, hydrazino), 9.47 (s, 1H, NH proton); ¹³C NMR (DMSO-d₆, 400 MHz) δ 20.58 (CH₃ at C₅ of indolyl), 56.69 (2C, C₃, C₅ of morpholyl), 58.8 (2C, C₂, C₆ of morpholyl), 62.14 (–CH₂–), 65.37 (CH₃ of methoxythiosemicarb), 115.67 (C₇ of indolyl), 124.39 (C₅ of indolyl), 126.14 (C₆ of indolyl), 129.23 (C_{4a} of indolyl), 129.42 (C₄ of indolyl), 136.07 (C₃ of indolyl), 148.79 (C_{7a} of indolyl), 155.39 (C₂ of indolyl), 158.93 (C of carbothioamido); Anal[calculated/found]. C, 52.88/53.09; H, 5.82/5.83; N, 19.27/19.21; C₁₆H₂₁N₅O₃S

6.1.3.19. 2-(5-Chloro-2-oxo-1-[[4-phenyltetrahydropyrazin-1(2H)-yl]methyl]-1,2-dihydro-3H-indol-3-yliden)-N-(methoxy)hydrazine-1-carbothioamide (**B16**). %Yield: 93.33; M.P: 80–82 °C; ¹H NMR (DMSO-d₆, 400 MHz) δ 3.15 (t, 4H, C₂, C₆ of piperaziny), 3.18 (t, 4H, C₃, C₅ of piperaziny), 3.43 (s, 3H, methoxyl), 5.15 (s, 2H, –NCH₂N–), 6.73 (d, 2H, C₂, C₆ of phenyl), 6.83 (d, 1H, C₄ of phenyl), 6.81(d, 1H, C₇ of indolyl), 7.21 (m, 2H, C₃, C₅ of phenyl), 7.25 (d, 1H, C₆ of indolyl), 8.13 (s, 1H, C₄ of indolyl), 8.53 (s, 1H, hydrazino), 9.46 (s, 1H, hydroxyl); ¹³C NMR (DMSO-d₆, 400 MHz) δ 48.17 (2C, C₃, C₅ of piperaziny), 51.73 (2C, C₂, C₆ of piperaziny), 62.25 (–CH₂–), 65.37 (CH₃ of methoxy thiosem), 116.35 (2C, C₂, C₆ of phenyl), 118.45 (C₇ of indolyl), 120.3 (C₄ of Ph), 124.88 (C₄ of indolyl), 126.87 (C₅ of indolyl), 127.88 (C_{4a} of indolyl), 129.1 (2C, C₃, C₅ of Phenyl), 130.12 (C₆ of indolyl), 136.12 (C₃ of indolyl), 146.83 (C_{7a} of Indolyl), 150.73 (C₁ of Phenyl), 155.39 (C₂ of indolyl), 158.93 (C of carbothioamido); Anal[calculated/found]. C, 54.96/55.14; H, 5.05/5.03; N, 18.31/18.36; C₂₁H₂₃ClN₆O₂S.

6.1.3.20. 2-(5-Chloro-1-[[4-(4-chlorophenyl) tetrahydropyrazin-1(2H)-yl]methyl]-2-oxo-1,2-dihydro-3H-indol-3-yliden)-N-(methoxy)hydrazine-1-carbothioamide (**B19**). %Yield: 74.26; M.P: 208–210 °C; ¹H NMR (DMSO-d₆, 400 MHz) δ 3.17 (t, 4H, C₂, C₆ of piperaziny), 3.20 (t, 4H, C₃, C₅ of piperaziny), 3.51 (s, 3H, methoxyl), 5.13 (s, 2H, –NCH₂N–), 6.65 (d, 2H, C₂, C₆ of phenyl), 6.79 (d, 1H, C₇ of indolyl), 6.82 (m, 2H, C₃, C₅ of phenyl), 7.34 (d, 1H, C₆ of indolyl), 8.07 (s, 1H, C₄ of indolyl), 8.53 (s, 1H, hydrazino), 9.48 (s, 1H, NH proton); ¹³C NMR (DMSO-d₆, 400 MHz) δ 48.17 (2C, C₃, C₅ of pip), 51.73 (2C, C₂, C₆ of piperaziny), 62.25 (–CH₂–), 65.37 (CH₃ of methoxy thiosem), 118.45 (C₇ of indolyl), 124.84 (2C, C₂, C₆ of phenyl), 124.88 (C₄ of indolyl), 126.87 (C₅ of indolyl), 127.88 (C_{4a} of Indolyl), 127.93 (2C, C₃, C₅ of indolyl), 129.95 (C₄ of phenyl), 130.12 (C₆ of indolyl), 136.12 (C₃ of indolyl), 146.74 (C₁ of phenyl), 146.83 (C_{7a} of indolyl), 155.39 (C₂ of indolyl), 158.93 (C of carbothioamido); Anal[calculated/found]. C, 51.12/50.96; H, 4.49/4.49; N, 17.03/17.06; C₂₁H₂₂Cl₂N₆O₂S.

6.1.3.21. 2-(1-[[4-(4-Chlorophenyl)tetrahydropyrazin-1(2H)-yl]methyl]-5-methyl-2-oxo-1,2-dihydro-3H-indol-3-yliden)-N-(methoxy)hydrazine-1-carbothioamide (**B21**). %Yield: 85.46; M.P: 140 °C; ¹H NMR (DMSO-d₆, 400 MHz) δ 2.43 (s, 3H, CH₃), 3.18 (t, 4H, C₂, C₆ of piperaziny), 3.21 (t, 4H, C₃, C₅ of piperaziny), 3.57 (s, 3H, methoxyl), 5.09 (s, 2H, –NCH₂N–), 6.32 (d, 2H, C₂, C₆ of phenyl), 6.69 (d, 1H, C₇ of indolyl), 6.81 (m, 2H, C₃, C₅ of phenyl), 7.06 (d, 1H, C₆ of indolyl), 7.37 (s, 1H, C₄ of indolyl), 8.51 (s, 1H, hydrazino), 9.46 (s, 1H, NH proton); ¹³C NMR (DMSO-d₆, 400 MHz) δ 20.58 (CH₃ at C₅ of indolyl), 48.17 (2C, C₃, C₅ of piperaziny), 51.73 (2C, C₂, C₆ of piperaziny), 62.25 (–CH₂–), 65.37 (CH₃ of methoxy thiosem), 115.89 (C₇ of indolyl), 124.39 (C₅ of indolyl), 124.84 (2C, C₂, C₆ of phenyl), 126.14 (C₆ of indolyl), 127.93 (2C, C₃, C₅ of phenyl), 129.42 (C₄ of indolyl), 129.44 (C_{4a} of indolyl), 129.95 (C₄ of phenyl), 136.07 (C₃ of indolyl), 146.74 (C₁ of phenyl), 148.71 (C_{7a} of indolyl), 155.39 (C₂

of indolyl), 158.93 (C of carbothioamido); Anal[calculated/found]. C, 55.86/56.05; H, 5.33/5.35; N, 17.77/17.73; C₂₂H₂₅ClN₆O₂S.

6.1.3.22. 2-(5-Fluoro-1-[[4-[4-(methyloxy)phenyl]tetrahydropyrazin-1(2H)-yl]methyl]-2-oxo-1,2-dihydro-3H-indol-3-yliden)-N-(methyloxy)hydrazine-1-carbothioamide (**B23**). %Yield: 69.35; M.P: 116–118 °C; ¹H NMR (DMSO-*d*₆, 400 MHz) δ 3.14 (t, 4H, C₂, C₆ of piperazinyl), 3.19 (t, 4H, C₃, C₅ of piperazinyl), 3.59 (s, 3H, methoxy), 3.71 (s, 3H, 4-methoxy), 5.11 (s, 2H, -NCH₂N-), 6.15 (d, 2H, C₂, C₆ of phenyl), 6.47 (d, 1H, C₇ of indolyl), 6.57 (m, 2H, C₃, C₅ of phenyl), 7.23 (d, 1H, C₆ of indolyl), 7.73 (s, 1H, C₄ of indolyl), 8.51 (s, 1H, hydrazino), 9.47 (s, 1H, NH proton); ¹³C NMR (DMSO-*d*₆, 400 MHz) δ 48.17 (2C, C₃, C₅ of piperazinyl), 51.73 (2C, C₂, C₆ of phenyl), 55.2 (CH₃ of 4-methoxy phenyl), 62.25 (-CH₂-), 65.37 (CH₃ of methoxy thiosem), 112.82 (2C, C₃, C₅ of phenyl), 113.91 (C₄ of indolyl), 115.07 (C₆ of indolyl), 117.69 (C₇ of indolyl), 124.44 (2C, C₂, C₆ of phenyl), 128.27 (C_{4a} of indolyl), 133.61 (C₃ of indolyl), 142.19 (C₁ of phenyl), 145.62 (C_{7a} of phenyl), 147.57 (C₅ of indolyl), 155.39 (C₂ of indolyl), 157.24 (C₄ of phenyl), 158.93 (C of carbothioamido); Anal[calculated/found]. C, 55.92/55.78; H, 5.33/5.31; N, 17.78/17.82; C₂₂H₂₅FN₆O₃S.

6.1.3.23. 1-Ethyl-6-fluoro-7-[4-[[5-fluoro-3-((Z)-2-[(methyloxy)amino]carbothioyl]hydrazono)-2-oxo-1H-indol-1(2H)-yl]methyl]tetrahydropyrazin-1(2H)-yl]-4-oxo-1,4-dihydroquinoline-3-carboxylic acid (**B26**). %Yield: 93.50; M.P: 66–68 °C; ¹H NMR (DMSO-*d*₆, 400 MHz) δ 1.21 (t, 3H, CH₃ of C₂H₅), 3.13 (t, 4H, C₂, C₆ of piperazinyl), 3.16 (t, 4H, C₃, C₅ of piperazinyl), 3.62 (s, 2H, methylene), 4.31 (q, 2H, CH₂ of C₂H₅), 6.23 (s, 1H, C₈ of quinoliny), 6.61 (s, 3H, methoxy), 7.21 (s, 1H, C₅ of quinoliny), 7.29 (d, 1H, C₆ of indolyl), 7.31 (s, 1H, C₂ of quinoliny), 7.73 (s, 1H, C₄ of indolyl), 8.52 (s, 1H, hydrazine), 9.49 (s, 1H, NH proton), 10.53 (s, 1H, carboxylate); ¹³C NMR (DMSO-*d*₆, 400 MHz) δ 14.4 (CH₃ of C₂H₅ at N₁ of quinoliny), 49.01 (CH₂ of C₂H₅), 50.02 (2C, C₃, C₅ of piperazinyl), 51.73 (2C, C₂, C₆ of piperazinyl), 62.25 (-CH₂-), 65.37 (CH₃ of methoxy thiosem), 106.84 (C₈ of quinoliny), 107.04 (C₃ of quinoliny), 111.2 (C₅ of quinoliny), 113.91 (C₄ of indolyl), 115.07 (C₆ of indolyl), 117.69 (C₇ of indolyl), 119.8 (C_{4a} of quinoliny), 128.27 (C_{4a} of indolyl), 133.61 (C₃ of indolyl), 136.9 (C_{8a} of quinoliny), 143.37 (C₇ of quinoliny), 145.62 (C_{7a} of indolyl), 147.57 (C₅ of indolyl), 148.4 (C₂ of quinoliny), 152.83 (C₆ of quinoliny), 155.39 (C₂ of indolyl), 158.93 (C of carbothioamido), 165.6 (C of COOH), 175.8 (C₄ of quinoliny); Anal[calculated/found]. C, 54.08/54.23; H, 4.54/4.56; N, 16.35/16.38; C₂₇H₂₇F₂N₇O₅S.

6.1.3.24. 7-[4-[[5-chloro-3-((Z)-2-[(methyloxy)amino]carbothioyl]hydrazono)-2-oxo-1H-indol-1(2H)-yl]methyl]tetrahydropyrazin-1(2H)-yl]-1-cyclopropyl-6-fluoro-4-oxo-1,4-dihydroquinoline-3-carboxylic acid (**B28**). %Yield: 72.53; M.P: 128–130 °C (d); ¹H NMR (DMSO-*d*₆, 400 MHz) δ 0.39 (m, 4H, CH₂ of cyclopropyl), 2.51 (t, 1H, CH of cyclopropyl), 2.95 (t, 4H, C₃, C₅ of piperazinyl), 3.13 (t, 4H, C₂, C₆ of piperazinyl), 3.61 (s, 3H, methoxy), 5.09 (s, 2H, methylene), 6.43 (s, 1H at C₈ of quinoliny), 6.67 (d, 1H at C₇ of indolyl), 6.95 (s, 1H at C₅ of quinoliny), 7.16 (d, 1H at C₆ of indolyl), 7.54 (s, 1H at C₂ of quinoliny), 7.72 (s, 1H at C₄ of indolyl), 8.51 (s, 1H, hydrazine), 9.46 (s, 1H, NH proton), 11.03 (s, 1H, carboxylate); ¹³C NMR (DMSO-*d*₆, 400 MHz) δ 7.7 (2C, CH₂ of cyclopropyl), 30.6 (CH of cyclopropyl), 50.02 (2C, C₃, C₅ of piperazinyl), 51.73 (2C, C₂, C₆ of piperazinyl), 62.25 (-CH₂-), 65.37 (CH₃ of methoxy thiosem), 99.43 (C₈ of quinoliny), 103.6 (C₅ of quinoliny), 107.6 (C₃ of quinoliny), 112.3 (C_{4a} of quinoliny), 118.45 (C₇ of indolyl), 124.88 (C₄ of indolyl), 126.87 (C₅ of indolyl), 127.88 (C_{4a} of indolyl), 130.12 (C₆ of indolyl), 133.01 (C_{8a} of indolyl), 136.12 (C₃ of indolyl), 139.76 (C₇ of quinoliny), 140.9 (C₂ of quinoliny), 146.83 (C_{7a} of indolyl), 148.43 (C₆ of quinoliny), 155.39 (C₂ of indolyl), 158.93 (C of carbothioamido), 161.9 (C of COOH), 177.5 (C₄ of quinoliny); Anal[calculated/found]. C, 53.54/53.71; H, 4.33/4.35; N, 15.61/15.64; C₂₈H₂₇ClFN₇O₅S.

6.1.3.25. 1-Cyclopropyl-6-fluoro-7-[4-[[5-methyl-3-((Z)-2-[(methyloxy)amino]carbothioyl]hydrazono)-2-oxo-1H-indol-1(2H)-yl]methyl]tetrahydropyrazin-1(2H)-yl]-4-oxo-1,4-dihydroquinoline-3-carboxylic acid (**B30**). %Yield: 85.67; M.P: 150–154 °C (d); ¹H NMR (DMSO-*d*₆, 400 MHz) δ 0.43 (m, 4H, CH₂ of cyclopropyl), 2.48 (s, 3H, methyl at C₅ of indolyl), 2.53 (t, 1H, CH of cyclopropyl), 3.11 (t, 4H, C₂, C₆ of piperazinyl), 3.18 (t, 4H, C₃, C₅ of piperazinyl), 3.61 (s, 3H, methoxy), 5.13 (s, 2H, methylene), 6.43 (s, 1H at C₈ of quinoliny), 6.67 (d, 1H at C₇ of indolyl), 6.95 (s, 1H at C₅ of quinoliny), 7.16 (d, 1H at C₆ of indolyl), 7.54 (s, 1H at C₂ of quinoliny), 7.72 (s, 1H at C₄ of indolyl), 8.53 (s, 1H, hydrazine), 9.47 (s, 1H, NH proton), 11.34 (s, 1H, carboxylate); ¹³C NMR (DMSO-*d*₆, 400 MHz) δ 7.7 (2C, CH₂ of cyclopropyl), 20.58 (CH₃ at C₅ of indolyl), 30.6 (CH of cyclopropyl), 50.02 (2C, C₃, C₅ of piperazinyl), 51.73 (2C, C₂, C₆ of piperazinyl), 62.25 (-CH₂-), 65.37 (CH₃ of methoxy thiosem), 99.43 (C₈ of quinoliny), 103.6 (C₅ of quinoliny), 107.6 (C₃ of quinoliny), 112.3 (C_{4a} of quinoliny), 115.89 (C₇ of indolyl), 124.39 (C₅ of indolyl), 126.14 (C₆ of indolyl), 129.42 (C₄ of indolyl), 129.44 (C_{4a} of indolyl), 136.07 (C₃ of indolyl), 139.76 (C₇ of quinoliny), 140.9 (C₂ of quinoliny), 148.43 (C₆ of quinoliny), 148.71 (C_{7a} of quinoliny), 155.39 (C₂ of indolyl), 158.93 (C of carbothioamido), 161.9 (C of COOH), 177.5 (C₄ of quinoliny); Anal[calculated/found]. C, 57.32/57.23; H, 4.98/4.99; N, 16.14/16.11; C₂₉H₃₀FN₇O₅S.

6.1.3.26. 1-Ethyl-6,8-difluoro-7-[4-[[5-fluoro-3-((Z)-2-[(methyloxy)amino]carbothioyl]hydrazono)-2-oxo-1H-indol-1(2H)-yl]methyl]-3-methyltetrahydropyrazin-1(2H)-yl]-4-oxo-1,4-dihydroquinoline-3-carboxylic acid (**B32**). %Yield: 72.90; M.P: 180 °C (d); ¹H NMR (DMSO-*d*₆, 400 MHz) δ 0.94 (d, 3H, methyl at C₃ of piperazinyl), 1.21 (t, 3H, CH₃ of C₂H₅), 2.85 (d, 2H, C₂ of piperazinyl), 3.14 (t, 2H, C₆ of piperazinyl), 3.21 (m, 1H, C₃ of piperazinyl), 3.56 (t, 2H, C₅ of piperazinyl), 3.61 (s, 3H, methoxy), 4.32 (q, 2H, CH₂ of C₂H₅), 5.13 (s, 2H, methylene), 6.57 (d, 1H, C₇ of indolyl), 7.19 (s, 1H, C₅ of quinoliny), 7.31 (d, 1H, C₆ of indolyl), 7.52 (s, 1H, C₂ of quinoliny), 7.71 (s, 1H, C₄ of indolyl), 8.51 (s, 1H, hydrazine), 9.46 (s, 1H, NH proton), 10.74 (s, 1H, carboxylate); ¹³C NMR (DMSO-*d*₆, 400 MHz) δ 15.7 (CH₃ of C₂H₅), 18.12 (CH₃ at C₃ of piperazinyl), 46.7 (CH₂ of C₂H₅), 52.38 (C₆ of piperazinyl), 52.88 (C₅ of piperazinyl), 57.64 (C₃ of piperazinyl), 60.04 (-CH₂-), 62.35 (C₂ of piperazinyl), 65.37 (C of methoxy thiosem), 105.99 (C₅ of quinoliny), 107 (C₃ of quinoliny), 113.91 (C₄ of indolyl), 115.07 (C₆ of indolyl), 117.69 (C₇ of indolyl), 121.2 (C_{4a} of quinoliny), 126.39 (C₇ of quinoliny), 128.27 (C_{4a} of indolyl), 131.49 (C_{8a} of quinoliny), 133.61 (C₃ of indolyl), 140.88 (C₈ of quinoliny), 143.89 (C₆ of quinoliny), 145.28 (C_{7a} of indolyl), 147.57 (C₅ of indolyl), 151.01 (C₂ of quinoliny), 155.39 (C₂ of indolyl), 158.93 (C of carbothioamido), 165.03 (C of COOH), 174.2 (C₄ of quinoliny); Anal[calculated/found]. C, 53.24/53.17; H, 4.47/4.48; N, 15.52/15.46; C₂₈H₂₈F₃N₇O₅S.

6.1.3.27. 1-Cyclopropyl-6-fluoro-7-[4-[[5-fluoro-3-((Z)-2-[(methyloxy)amino]carbothioyl]hydrazono)-2-oxo-1H-indol-1(2H)-yl]methyl]-3-methyltetrahydropyrazin-1(2H)-yl]-8-(methyloxy)-4-oxo-1,4-dihydroquinoline-3-carboxylic acid (**B35**). %Yield: 70.23; M.P: 88–90 °C; ¹H NMR (DMSO-*d*₆, 400 MHz) δ 0.41 (m, 4H, CH₂ of cyclopropyl), 0.93 (d, 3H, methyl at C₃ of piperazinyl), 2.45 (t, 1H, CH of cyclopropyl), 2.87 (d, 2H, C₂ of piperazinyl), 3.12 (t, 2H, C₆ of piperazinyl), 3.21 (m, 1H, C₃ of piperazinyl), 3.53 (t, 2H, C₅ of piperazinyl), 3.57 (s, 3H, methoxy), 3.61 (s, 3H, methoxy at C₈ of quinoliny), 5.12 (s, 2H, methylene), 6.59 (d, 1H, C₇ of indolyl), 7.25 (d, 1H, C₆ of indolyl), 7.31 (s, 1H, C₅ of quinoliny), 7.38 (s, 1H, C₂ of quinoliny), 7.72 (s, 1H, C₄ of indolyl), 8.52 (s, 1H, hydrazine), 9.47 (s, 1H, NH proton), 10.66 (s, 1H, carboxylate); ¹³C NMR (DMSO-*d*₆, 400 MHz) δ 7.7 (2C, CH₂ of cyclopropyl), 18.12 (CH₃ at C₃ of piperazinyl), 31.97 (CH of cyclopropyl), 50.88 (C₆ of piperazinyl), 52.88 (C₅ of piperazinyl), 57.64 (C₃ of piperazinyl), 57.77 (methoxy C at C₈ of

quinoliny), 60.04 (–CH₂–), 60.85 (C₂ of piperaziny), 65.37 (C of methoxy thiosem), 102.56 (C₅ of quinoliny), 107.04 (C₃ of quinoliny), 113.91 (C₄ of indoly), 115.07 (C₆ of indoly), 117.69 (C₇ of indoly), 122.43 (C_{4a} of quinoliny), 122.88 (C_{8a} of quinoliny), 128.27 (C_{4a} of indoly), 132.29 (C₇ of quinoliny), 133.61 (C₃ of indoly), 142.76 (C₈ of quinoliny), 145.28 (C_{7a} of quinoliny), 146.39 (C₂ of quinoliny), 147.57 (C₅ of indoly), 155.07 (C₆ of quinoliny), 155.39 (C₂ of indo), 158.93 (C of carbothioamido), 163.68 (C of COOH), 174.28 (C₄ of quinoliny); Anal[calculated/found]. C, 54.95/55.12; H, 4.77/4.78; N, 14.95/14.98; C₃₀H₃₁F₂N₇O₆S.

6.1.3.28. 1-Cyclopropyl-6-fluoro-7-[3-methyl-4-[[5-methyl-3-((Z)-2-[[[(methyloxy)amino]carbothioyl]hydrazono)-2-oxo-1H-indol-1(2H)-yl]methyl]tetrahydropyrazin-1(2H)-yl]-8-(methyloxy)-4-oxo-1,4-dihydroquinoline-3-carboxylic acid (B36). %Yield: 46.09; M.P: 70–72 °C; ¹H NMR (DMSO-*d*₆, 400 MHz) δ 0.41 (m, 4H, CH₂ of cyclopropyl), 0.93 (d, 3H, methyl at C₃ of piperaziny), 2.38 (s, 3H, C₅ of indoly), 2.45 (t, 1H, CH of cyclopropyl), 2.87 (d, 2H, C₂ of piperaziny), 3.12 (t, 2H, C₆ of piperaziny), 3.21 (m, 1H, C₃ of piperaziny), 3.53 (t, 2H, C₅ of piperaziny), 3.57 (s, 3H, methoxy), 3.61 (s, 3H, methoxy at C₈ of quinoliny), 5.12 (s, 2H, methylene), 6.59 (d, 1H, C₇ of indoly), 7.25 (d, 1H, C₆ of indoly), 7.31 (s, 1H, C₅ of quinoliny), 7.38 (s, 1H, C₂ of quinoliny), 7.72 (s, 1H, C₄ of indoly), 8.53 (s, 1H, hydrazine), 9.45 (s, 1H, NH proton), 11.37 (s, 1H, carboxylate); ¹³C NMR (DMSO-*d*₆, 400 MHz) δ 7.7 (2C, CH₂ of cyclopropyl), 18.12 (CH₃ at C₃ of piperaziny), 20.58 (CH₃ at C₅ of indoly), 31.97 (CH of cyclopropyl), 50.88 (C₆ of piperaziny), 52.88 (C₅ of piperaziny), 57.64 (C₃ of piperaziny), 57.77 (methoxy C at C₈ of quinoliny), 60.04 (–CH₂–), 60.85 (C₂ of piperaziny), 65.37 (C of methoxy thiosem), 102.56 (C₅ of quinoliny), 107.03 (C₃ of quinoliny), 115.89 (C₇ of indoly), 122.43 (C_{4a} of quinoliny), 122.88 (C_{8a} of quinoliny), 124.39 (C₅ of indoly), 126.14 (C₆ of indoly), 129.42 (C₄ of indoly), 129.44 (C_{4a} of indoly), 136.07 (C₃ of indoly), 132.29 (C₇ of quinoliny), 142.76 (C₈ of quinoliny), 146.39 (C₂ of quinoliny), 147.91 (C_{7a} of indoly), 155.07 (C₆ of quinoliny), 155.39 (C₂ of indoly), 158.93 (C of carbothioamido), 163.68 (C of COOH), 174.28 (C₄ of quinoliny); Anal[calculated/found]. C, 57.13/56.97; H, 5.26/5.28; N, 15.04/15.02; C₃₁H₃₄N₇O₆S.

6.2. Biological activity

6.2.1. Anti-HIV activity

The compounds were evaluated for their anti-HIV activity and cytotoxicity against replication of HIV-1 strain III_B in MT-4 cells using the 3-(4, 5-dimethylthiazol-2-yl)-2,5-diphenyltetrazolium bromide (MTT) assay method. The MT-4 cells were grown in RPMI-1640 DM (Dutch modification) medium (Flow lab, Irvine Scotland), supplemented with 10% v/v heat-inactivated calf serum and 20 µg/mL gentamicin (E. Merck Darmstadt, Germany). HIV-1 (IIIB) was obtained from the culture supernatant of HIV-1 infected MT-4 cell lines and the virus stocks were stored at –70 °C until used. Anti-HIV assays were carried out in microtitre plates filled with 100 µL of medium and 25 µL volumes of compounds in triplicate so as to allow simultaneous evaluation of their effects on HIV- and mock-infected cells. 50 µL of HIV at 100 CCID₅₀ (50% cell culture infective dose) medium were added to either the HIV-infected or mock-infected part of the microtitre tray. Cultures were incubated at 37 °C in a humidified atmosphere at 5% CO₂ in atmosphere for five days. The viability of mock and HIV-infected cells was examined spectrophotometrically to assess the anti-HIV activity and cytopathic effect of the test compounds [26].

6.2.2. HIV-1 RT enzyme inhibition assay

The assay protocol involved a reaction mixture (50 µL) comprising of 50 mM tris-HCl (pH 7.8), 5 mM dithiothreitol, 30 mM glutathione, 50 µM EDTA, 150 mM KCl, 5 mM MgCl₂, 1.25 µg bovine serum

albumin, an appropriate concentration of radiolabelled substrate [³H] dGTP, 0.1 mM poly (vC)-oligo (dG) as the template/primer, 0.06% Triton X-100, 10 µL of inhibitor solution (containing various concentrations of compounds), and 1 µL of RT preparation. The reaction mixtures were incubated for 15 min at 37 °C, after which 100 µL of calf thymus DNA (150 µg/mL), 2 mL of Na₄P₂O₇ (0.1 M in 1 M HCl), and 2 mL of trichloroacetic acid (10 %v/v) were added. The solutions were kept on ice for 30 min, after which the acid-insoluble material was washed and analyzed for radioactivity. For the experiments in which 50% inhibitory concentration (IC₅₀) of the test compounds was determined, fixed concentration of 2.5 µ [³H] dGTP was used [26].

6.2.3. In-vitro anti-tubercular activity in log phase cultures

All compounds were screened for their in vitro anti-mycobacterial activity against log phase cultures of MTB in Middlebrook 7H11 agar medium supplemented with OADC by agar dilution method similar to that recommended by the National Committee for Clinical Laboratory Standards for the determination of MIC in triplicate. The MIC is defined as the minimum concentration of compound required to produce complete inhibition of bacterial growth [27].

6.2.4. In-vitro anti-tubercular activity in 6 week starved cultures

For starvation experiments, MTB cells were grown in Middlebrook 7H9 medium supplemented with 0.2% (v/v) glycerol, 10% (v/v) Middlebrook oleic acid-albumin-dextrose-catalase (OADC) enrichment, and 0.025% (v/v) Tween 80 at 37 °C with constant rolling at 2 rpm until they reached an optical density at 600 nm of ~ 0.6. The cells were then washed twice and re-suspended in phosphate-buffered saline (PBS) at the same cell density. Cells (50 mL of culture) were incubated at 37 °C for an additional 6 weeks in 1-L roller bottles. Compounds, dissolved in DMSO, were added to either 1 mL PBS containing ~ 1 × 10⁷ starved MTB cells at various concentrations. Cultures were incubated in 15-mL conical tubes at 37 °C with constant shaking for 7 days and then washed twice in PBS before dilutions were plated on Middlebrook 7H11 plates supplemented with 0.2% (v/v) glycerol, 10% (v/v) Middlebrook OADC enrichment, and 0.025% (v/v) Tween 80, containing no antibiotics. Bacterial growth was determined after incubation for 4 weeks at 37 °C. The MIC is defined as the minimum concentration of compound which brings about complete inhibition of bacterial growth. All values were determined in triplicate [28].

6.2.5. MTB ICL enzyme assay

Isocitrate lyase activity was determined at 37 °C by measuring the formation of glyoxylate-phenylhydrazone at 324 nm. The reaction mixture contains 100 µL of 0.5 mM potassium phosphate buffer, 1.2 µL of 1 mM magnesium chloride, 24 µL of 100 mM 2-mercaptoethanol, 7 µL of 4 mM phenylhydrazine hydrochloride, 6 µL of 50 mM trisodium isocitric acid and ICL enzyme (usually 3–6 µL). This mixture is made up to 200 µL with MilliQ water. At the end of the 10th minute this reaction mixture is made up to 1 mL and UV absorbance is measured at 324 nm which serves as a control. For the test compounds 3 µL of 100 mM 3-NPA was used and in case of the candidate molecules 10 µL of 10 mM concentration were added with the above mentioned reaction mixture. At the end of the 10th minute this reaction mixture is made up to 1 mL and UV absorbance is measured at 324 nm which serves as a test. The % inhibition is calculated by the formulae control absorbance minus test absorbance divided by control absorbance multiplied by 100.

6.3. Computational methodology

6.3.1. 3D-qsar analysis

The molecular modeling studies namely, CoMFA, Advanced CoMFA and CoMSIA were performed using SYBYL6.9 molecular

modeling software running on a Silicon Graphics Octane R12000³⁸ workstation. The structures were built in 2D using MDL ISIS Draw 2.5 software, and were imported to Discovery Studio 2.0 (Catalyst) software. CHARMM force field was applied to the molecules and later energy minimized. These 3D structures were then exported to the SYBYL6.9 workstation where partial charges were calculated using Gasteiger–Hückel method geometry optimized using Tripos force field with a distance-dependent dielectric function until a root mean square deviation (RMSD) of 0.01 kcal/mol Å was achieved. Two different alignment techniques viz. (a) common substructure fitting method and (b) manual alignment method were compared to obtain the most efficient alignment for this set of structurally diverse molecules. The common substructure fitting method involves superimposition of all the molecules to a common substructure of the template molecule. In the manual method, the molecules were aligned manually over a template molecule. Amongst the two, manual alignment method gave better results.

6.3.1.1. Data sets. A set of fifty-four molecules, characterized by a central 2-hydroxy/methoxy carbamothioyl hydrazine carboxamide moiety, was divided into a training set and a test set taking into account either the structural aspects or the anti-HIV inhibitory profile of compounds. The training set was chosen according to these criterions: (i) the most- and least-active compounds were both included.; (ii) compounds were chosen in such a way that the entire activity range was uniformly sampled; and (iii) structural superfluity was avoided selecting compounds with different substituents or substitution patterns.

6.3.1.2. CoMFA studies. The CoMFA calculations were done using Tripos Standard and Advanced CoMFA modules in SYBYL. For each alignment, an sp³ carbon atom having a charge of +1 and a radius of 1.52 Å was used as a probe to calculate various steric and electrostatic fields, the grid spacing was set to 2 Å and the region was calculated automatically. To investigate the influence of different parameter settings on CoMFA, various steric and electrostatic cutoffs and grid spacing were set to 30 kcal/mol [29].

6.3.1.3. Advanced CoMFA. H-bonding, indicator and parabolic fields were used in the Advanced CoMFA routine. Lattice points with steric energies below the steric cutoff energy were assigned nominal energies equal to the steric cutoff energies if they were close to H-bond accepting or donating atoms. Indicator fields replaced all lattice energies with magnitudes below a designated threshold with zero values. All energies at or above that threshold were replaced with a nominal energy equal in magnitude to the relevant field cutoff value. When both fields were included in a single CoMFA column, the greater of the steric and electrostatic cutoffs was used. The sign of the original lattice energy is retained. Parabolic fields are those in which the magnitude of a standard steric and/or electrostatic field at each lattice point has been squared; the original sign of the energy is retained.

6.3.1.4. CoMFA region focusing. CoMFA region focusing is a method of application of weights to the lattice points in a CoMFA region to enhance or attenuate the contribution of these points to subsequent analysis. In this study, discriminant power values as weights and different factors were applied in addition to grid spacing for getting better models.

6.3.1.5. CoMSIA studies. Five similarity fields namely, steric, electrostatic, and hydrophobic, hydrogen bond donor and acceptor were calculated. The lattice dimensions were selected with a sufficiently large margin extended up to 4 Å surrounding all aligned molecules. In CoMSIA, the steric indices are related to the third

power of the atomic radii, the electrostatic descriptors are derived from atomic partial charges, the hydrophobic fields are derived from atom-based parameters, and the hydrogen bond donor and acceptor indices are obtained by a rule-based method derived from experimental values. In the present work, similarity indices were computed using a probe atom with radius 1.0 Å, charge +1, hydrophobicity +1, hydrogen bond donor and acceptor properties of +1 and attenuation factor of 0.3 for the Gaussian type distance function [30].

6.3.1.6. Validation of models. PLS analysis was used to correlate the activities with CoMFA and CoMSIA values containing the steric and electrostatic potentials. The models were cross-validated using the Leave One Out (LOO) method by SAMPLS method. The LOO method involves excluding one compound from the data set and then deriving a model using the rest. Then with the help of this derived model, the activity of the excluded molecule is determined. CoMFA standard scaling was applied to all the CoMFA analyses. The full PLS analysis was run with a column filtering of 2.0 kcal/mol to reduce the noise and to speed up the calculations. In case of CoMSIA as well, SAMPLS method was used. This was followed by a full PLS analysis, which was run using column filtering of 2.0 kcal/mol. Autoscaling was applied to all CoMSIA analyses.

6.3.2. Docking calculations onto HIV-1 RT

A crystallographic structure of HIV-1 RT in complex with nevirapine (PDB code 1VRT) [31] was used as protein starting structure for the docking simulation. Each inhibitor was built using Schrodinger Maestro and energy minimized in the same program and then docked onto RT using GOLD with the active site being defined using active atoms generated while redocking nevirapine onto HIV-1 RT. All the water molecules and the metal ions were removed from the protein structure prior to docking. Fifty genetic algorithms were performed for each ligand, with 100 000 energy evaluations.

6.3.3. Docking calculations onto MTB ICL

Three dimensional coordinates of the MTB ICL/BP complex (RCSB PDB entry 1F8M) [32] were used as the input structure for docking simulations performed on Autodock 4.0 due to the highly rigid structure of the molecule. The cocrystallized ligand was deleted from the protein structure. The protein was prepared using Schrodinger's protein preparation wizard only for hydrogen minimization. Schrodinger Maestro was used for ligand building and energy minimization and saved in *.mol format and then imported to Autodock 4.0. Grids of molecular interactions were considered in a cubic box of 50 × 50 × 50 with grid spacing of 0.375 Å. The active site was centred around the coordinate 19.4465, 41.903, 53.181. Few of the residues were assigned flexibility. Docking was performed 50 times using the Lamarckian genetic algorithm and a maximum of 250 000 energy evaluations. The final docked conformations were ranked according to their binding free energy.

Acknowledgment

This work was supported by grants from the Indian Council of Medical Research, New Delhi, India (58/9/2003-BMS) and University Grant Commission [F.No. 36-61/2008 (SR)], Government of India.

References

- [1] 2008 Report on the global AIDS epidemic. [Online] Available from: URL: www.unaids.org (2008).

- [2] Global tuberculosis control. WHO report 2008. [Online] Available from: URL: http://www.who.int/tb/publications/global_report/2008/en/index.html (2008).
- [3] D.J. Pepper, G.A. Meintjes, H. McIlleron, R. Wilkinson, J. Drug Discov. Today 12 (2007) 980–989.
- [4] M. Narita, D. Ashkin, E.S. Hollender, A.E. Pitchenik, Am. J. Respir. Crit. Care Med. 158 (1998) 157–161.
- [5] N.M. Parrish, J.D. Dick, W.R. Bishai, Trends Microbiol. 6 (1998) 107–112.
- [6] V. Sharma, S. Sharma, K. Hoener zu Bentrup, J.D. McKinney, D.G. Russell, W.R. Jacobs Jr., J.C. Sacchettini, Nat. Struct. Biol. 7 (2000) 663–668.
- [7] E. Katz, Rev. Clin. Basic Pharm. 6 (1987) 119–130.
- [8] J.A. Cooper, B. Moss, E. Katz, Virology 96 (1979) 381–392.
- [9] S.E. Webber, J. Tikhe, S.T. Worland, S.A. Fuhrman, T.F. Hendrickson, D.A. Matthews, R.A. Love, A.K. Patick, J.W. Meador, R.A. Ferre, E.L. Brown, D.M. DeLisle, C.E. Ford, S.L. Binford, J. Med. Chem. 39 (1996) 5072.
- [10] D. Ronen, L. Sherman, S. Bar-nun, Y. Teitz, Antimicrob. Agents Chemother. 31 (1987) 1798–1802.
- [11] L.R. Chen, Y.C. Wang, Y.W. Lin, S.Y. Chou, S.F. Chen, L.T. Liu, Y.T. Wu, C.J. Kuo, T.S. Chen, S.H. Juang, Bioorg. Med. Chem. Lett. 15 (2005) 3058–3062.
- [12] Y. Teitz, D. Ronen, A. Vansover, T. Stematsky, J.L. Riggs, Antivir. Res. 24 (1994) 305–314.
- [13] T.R. Bal, B. Anand, P. Yogeeswari, D. Sriram, Bioorg. Med. Chem. Lett. 15 (2005) 4451–4455.
- [14] D. Sriram, T.R. Bal, P. Yogeeswari, J. Pharm. Pharm. Sci. 8 (2005) 565–577.
- [15] D. Sriram, T.R. Bal, P. Yogeeswari, Med. Chem. 1 (2005) 277–285.
- [16] D. Sriram, P. Yogeeswari, Prathiba Dakhla, P. Senthil Kumar, Debjani Banerjee, Bioorg. Med. Chem. Lett. 17 (2007) 1888–1893.
- [17] J. Ren, R. Esnouf, E. Garman, D. Somers, C. Ross, I. Kirby, J. Keeling, G. Darby, Y. Jones, D. Stuart, D. Stammers, Nat. Struct. Mol. Biol. 2 (1995) 293–302.
- [18] J. Ren, D.K. Stammers, Trends Pharmacol. Sci. 26 (2005) 4–7.
- [19] L.A. Kohlstaedt, J. Wang, J.M. Fiedman, P.A. Rice, T.A. Steitz, Science 256 (1992) 1783–1790.
- [20] R. Esnouf, J. Ren, C. Ross, Y. Jones, D. Stammers, D. Stuart, Nat. Struct. Mol. Biol. 2 (1995) 303–308.
- [21] J.D. McKinney, K. Höner zu Bentrup, E.J. Muñoz-Elias, A. Miczak, B. Chen, W.T. Chan, D. Swenson, J.C. Sacchettini, W.R. Jacobs Jr., D.G. Russell, Nature 46 (2000) 735–738.
- [22] Y. Zhang, Annu. Rev. Pharmacol. Toxicol. 45 (2005) 529–564.
- [23] H.D. Park, Mol. Microbiol. 48 (2003) 833–843.
- [24] K.H.Z. Bentrup, A. Miczak, D.L. Swenson, D.G. Russell, J. Bacteriol. 181 (1999) 7161–7167.
- [25] K. Das, P.J. Lewi, S.H. Hughes, E. Arnold, Prog. Biophys. Mol. Biol. 88 (2005) 209–231.
- [26] D. Sriram, T.R. Bal, P. Yogeeswari, Bioorg. Med. Chem. 12 (2004) 5865–5873.
- [27] National Committee for Clinical Laboratory Standards, Antimycobacterial Susceptibility Testing for Mycobacterium Tuberculosis. Proposed Standard M24-T. National Committee for Clinical Laboratory Standards, Villanova, PA, 1995.
- [28] Z. Xie, N. Siddiqi, E.R. Rubin, Antimicrob. Agents Chemother. 49 (2005) 4778–4780.
- [29] G. Klebe, U. Abraham, J. Med. Chem. 36 (1993) 70–80.
- [30] G. Klebe, U. Abraham, T. Mietzner, J. Med. Chem. 37 (1994) 4130–4146.
- [31] RCSB Protein Data Bank ID. 1VRT.
- [32] RCSB Protein Data Bank ID. 1F8M.